

HOMOGENEOUS BED ION EXCHANGE COLUMN
MODELS FOR ULTRAPURE WATER APPLICATIONS
AND SIMULATION OF ION EXCHANGE BEDS
IN SERIES

By

ASHWIN P GRAMOPADHYE

Bachelor of Engineering

University of Pune

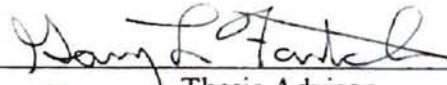
Maharashtra, India

1993

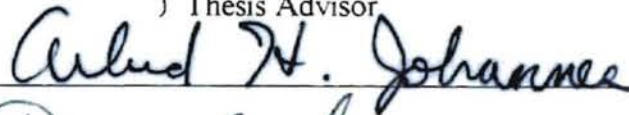
Submitted to the Faculty of the
Graduate College of the
Oklahoma State University
in partial fulfillment of
the requirements for
the Degree of
MASTER OF SCIENCE
December, 1996

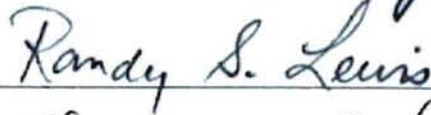
HOMOGENEOUS BED ION EXCHANGE COLUMN
MODELS FOR ULTRAPURE WATER APPLICATIONS
AND SIMULATION OF ION EXCHANGE BEDS
IN SERIES

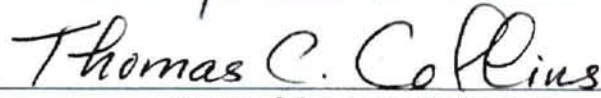
Thesis Approved



Thesis Advisor







Dean of Graduate College

PREFACE

This thesis deals with modeling of homogeneous-bed ion exchange under conditions of film-diffusion control for a multicomponent system of ions. A computer program to simulate ion-exchange columns in series is developed and used to compare the performance of homogeneous-bed trains with a mixed bed for equal ion-exchange capacities.

I am grateful to my advisor, Dr. Gary L. Foutch for his guidance, patience and inspiration throughout my study at Oklahoma State University. I would also like thank Dr. Arland H. Johannes and Dr. Randy Lewis for serving on my committee. I am indebted to Dr. J. D. Carlson (Department of Biosystems and Agricultural Engineering) for his encouragement and the interest he has shown in my well-being and progress. Working under Dr. J. D. Carlson and Dr. M. A. Kizer has been a great pleasure and has given me exposure to research in Agricultural Engineering -- a field new to me. Financial support from the School of Chemical Engineering and the Department of Biosystems and Agricultural Engineering is gratefully appreciated.

Special mention is due to my sister Chitra and parents Prabhakar and Geeta Gramopadhye for their love and emotional support. This study would not have been possible without their motivation and help. I also want to thank my friends Ram, Tara, Parag and Mandy for their encouragement and backing.

TABLE OF CONTENTS

Chapter		Page
I.	INTRODUCTION	1
	Ultrapure Water -- Role of Mixed Bed Ion Exchangers and Homogeneous Bed Ion Exchangers	2
	Objective	4
II.	LITERATURE REVIEW	6
	Applications of Homogeneous Bed Ion Exchangers	6
	Classification of Ion-Exchange Processes and Modeling Approaches	7
	Mechanism for Ion-Exchange Processes Involving Reactions	11
	Models for Homogeneous Bed Ion Exchange at Low Solution Concentrations	12
III	HOMOGENEOUS BED ION EXCHANGE MODEL	17
	Introduction	17
	Assumptions	18
	Ion-Exchange Equilibria	21
	Flux Expressions for Liquid-Film Diffusion	23
	Material Balance Equation for the Column	26
	Calculation of Temperature Dependent Parameters	27
	Comparison of Material Balance Equations in MBIE and HBIE.....	29
	Simulation of Homogeneous Beds in Series	30
IV.	HOMOGENEOUS BEDS VERSUS MIXED BEDS	32
	Abstract	32
	Introduction	32
	Feed Water Conditions, Resin Properties and Bed Parameters	33
	Results and Discussion	36
	Discussion on Breakthrough Curves	37
	Discussion on pH of Effluents	50
	Conclusions	60

BIBLIOGRAPHY	62
APPENDICES	65
APPENDIX A – INTERFACIAL CONCENTRATIONS AND ION-EXCHANGE EQUILIBRIA	65
APPENDIX B – MODEL EQUATIONS	68
APPENDIX C – MATERIAL BALANCE EQUATIONS	77
APPENDIX D – NUMERICAL METHODS	82
APPENDIX E – SIMULATION OF HOMOGENEOUS BEDS IN SERIES	84
APPENDIX F – COMPUTER CODE	86

LIST OF TABLES

Table		Page
I.	Classification of Ion-Exchange Processes Based on Nature of Interacting Resin and Electrolyte	8
II.	Classification of Ion-Exchange Processes Involving Reactions	10
III.	Assumptions for Derivation of Nernst-Planck Equation from Maxwell-Stefan Equation	15
IV.	Assumptions Made in the HBIE Model	20
V.	Algorithm for Interfacial Concentrations and Rates of Film Diffusion ...	25
VI.	Water Viscosity and Water Dissociation	27
VII.	Conductance as Function of Temperature	28
VIII.	Bed Parameters	35
IX.	Resin Properties	35
X.	Feed-Water Condition used in the Simulations	36

LIST OF FIGURES

Figure		Page
1	Solution Strategies for Differential Material Balance	30
2.	Schematic Diagram of Homogeneous Beds in Series and Mixed Bed	34
3.	Sodium Breakthrough for ACB, CAB and MB (High Concentrations)	38
4	Calcium Breakthrough for ACB, CAB and MB (High Concentrations)	40
5.	Sodium Breakthrough for ACB, CAB and MB (Low Concentrations)	42
6.	Calcium Breakthrough for ACB, CAB and MB (Low Concentrations)	43
7.	Chloride Breakthrough for ACB, CAB and MB (High Concentrations) ...	45
8.	Sulfate Breakthrough for ACB, CAB and MB (High Concentrations)	46
9.	Chloride Breakthrough for ACB, CAB and MB (Low Concentrations)	47
10.	Sulfate Breakthrough for ACB, CAB and MB (Low Concentrations)	48
11.	pH of Effluent for ACB, CAB and MB (High Concentrations)	51
12.	pH History for ACB (High Concentrations)	53
13	pH History for CAB (High Concentrations)	54
14	pH of Effluent for ACB, CAB and MB (Low Concentrations)	56
15.	pH History for ACB (Low Concentrations)	58
16.	pH History for CAB (Low Concentrations)	59

NOMENCLATURE

a_s	surface area per unit volume of resin (L^{-1})
B_i	any parameter B related to ionic species i
C_i	concentration of ionic species i (meq/L^3)
C_i^*	concentration of ionic species i at the resin-liquid interface (meq/L^3)
C_i^0	concentration of ionic species i in bulk liquid (meq/L^3)
C_T	total equivalent concentration (meq/L^3)
d_p	particle diameter (L)
D_i	self-diffusivity of ionic species i (L^2/T)
D_e	effective diffusivity (L^2/T)
F	Faraday's constant (Coulombs/mole)
FR	volumetric flowrate (L^3/T)
FAR	fraction of anionic resin in a mixed bed of ion exchange resin
FCR	fraction of cationic resin in a mixed bed of ion exchange resin
J_i	flux of ionic species i in the liquid film ($meq/T L^2$)
k	mass transfer coefficient (L/T)
K_A^B	selectivity coefficient for ion A in resin replaced by B from solution
K_w	equilibrium constant for water dissociation
m	number of coions
N_i	relative valence of counterion i

n	number of counterions
P	an exponent derived from solution of the flux expressions
q_i	concentration of ionic species i in the resin (meq/L ³)
Q	total capacity of resin (meq/L ³)
R	universal gas constant
Re	Reynolds number
Sc	Schmidt number
T	Temperature (K)
t	time (T)
u_s	superficial fluid velocity of bulk liquid (L/T)
V	volume of resin in resin bed (L ³)
x_i	fractional concentration of ionic species i in solution phase
y_i	fractional concentration of ionic species i in resin phase
z_i	charge (valence) on counterion i
z_j	charge (valence) on coion j
z_y	mean valence of coion i

GREEK LETTERS

δ	thickness of liquid film surrounding resin bead (L)
ε	void fraction in the resin bed
ϕ	electric potential (ergs/coulomb)
λ	conductance (S.m/mole)
μ	viscosity of water (cp)
ρ	density (M/L ³)

τ	dimensionless time coordinate
ω	parameter set to +1 for cations and -1 for anions
ξ	dimensionless space coordinate

SUBSCRIPTS

A	ion leaving resin phase
B	ion entering the resin phase
i	counterions
j	coions
r	reference ion

SUPERSCRIPTS

over bar	any quantity related to species in the resin phase
*	any quantity at the interface between resin and liquid
f	any quantity in the feed
o	any quantity in the bulk liquid

CHAPTER I

INTRODUCTION

Ion exchange is the partition of charged species between different phases of a system. It is a stoichiometric process. Every ion removed from one phase is replaced by an equivalent amount of another ionic species resulting in an exchange of equal charges between the two phases. Each phase maintains its electroneutrality.

Ion exchange shares traits with other methods of separation as illustrated by the similarity between the methods used to quantify and study ion-exchange phenomena and the methods used in other separation sciences. For example, equilibrium curves can be used to calculate distribution between phases for ion exchange in a fashion similar to liquid-liquid extraction. Blumberg (1984) examined the application by analogy of concepts from liquid-liquid extraction to resin-liquid systems.

Ion-exchange materials may be classified on the basis of the matrix that carries the fixed charges. Thus we have the following types (Helfferich, 1962):

1. Mineral ion exchangers, e.g. zeolites,
2. Ion-exchange resins, e.g. phenol sulfonic resins,
3. Ion-exchange coals -- they can be used as cation exchangers due to the carboxylic acid groups. Some coals can be sulfonated into cation exchangers.

4. Liquid ion exchangers, where two immiscible liquids exchange ions, e.g. long chain aliphatic amines dissolved in liquid xylene can act as an anion exchanger when the solvent is dispersed in aqueous phase having exchangeable ions.
5. Other materials with ion exchange properties, e.g. keratin, alumina, etc. Some substances such as nut shell and olive pits can be sulfonated to make cation exchangers.

Ion-exchange resins consist of a crosslinked hydrocarbon matrix, with bonded acidic or basic groups. The matrix can be formed by polycondensation or addition polymerization reaction and the fixed ionic groups can be introduced in the monomer or in the polymer after crosslinking. Ion-exchange resins are used more often than the other materials listed above, due to their superior chemical and mechanical stability, higher ion-exchange capacity and higher rate of ion exchange as compared to the other materials.

Ultrapure Water -- Role of Mixed Bed Ion Exchangers and Homogeneous Bed Ion Exchangers

The term 'Ultrapure Water' denotes water with 1 ppb or less of ionic contaminants (Sadler, 1993). Equally low levels of particulate and microbial impurities are expected. Such water is required by power plants (Harfst, 1995), paper and pulp manufacturers, petroleum refineries, dialysis units in hospitals, pharmaceutical manufacturers (Golden, 1986), compact disc manufacturers, semiconductor manufacturing industry, etc. (Okouchi et al., 1994).

Mixed bed ion exchange (MBIE) uses a mixture of cation-exchange resin and anion-exchange resin. A fixed bed of such a mixture, with the aqueous phase flowing down the bed, has been the favorite method in industry for achieving ultrapurity. In this mode, cations and anions are removed simultaneously. The alternative is to use homogeneous bed ion exchange (HBIE) where beds of cation and anion exchange resins are separate stages.

The advantage of MBIE over HBIE is that MBIE provides more separation zones in less volume -- very similar to having several stages of homogeneous cation and anion exchange beds of very small depth alternating with each other in series. The cation and anion resins replace the cations and anions, with hydrogen ions and hydroxide ions respectively, which then combine to form water. The simultaneous removal of cations and anions leads to a net reduction in ionic concentration in the bulk solution. Thus, there is a localized equilibrium within the bed, and consequently we get a very high separation efficiency. The net reduction in ionic concentration offers a distinctive advantage over HBIE where demineralization becomes progressively difficult with the removal of just cations or anions in a bed. For example, consider a cation-exchange bed followed by an anion-exchange bed. The effluent from the cation-exchange bed is acidic and goes to the anion-exchange bed. Anion exchange is thus highly favorable at the inlet. However, with progressing anion exchange, equilibrium becomes limiting and exchange is less favorable. Thus, the separation factor decreases sharply with progressive anion exchange.

Net reduction in ionic charge was the primary justification for use of MBIE as opposed to HBIE in ultrapure-water facilities in industry. However, resin regeneration presents two problems for MBIE, namely,

1. separation of cation exchange resin from anion exchange resin prior to regeneration and
2. remixing the resins uniformly after regeneration.

No such separation and remixing are required in HBIE. This represents one of the biggest advantages of HBIE over MBIE. The other problem encountered in MBIE is deterioration of anion exchange resin due to organic foulants in the feed water (Fisher, 1993). Cation resin is less susceptible to organic fouling as compared with anion resin and the cation resin can adsorb organic foulants without affecting resin performance drastically. Thus, the problem of anion resin fouling by organics in feed water can be ameliorated in HBIE by installing the cation resin bed ahead of the anion bed. These advantages have stimulated redevelopment of homogeneous bed techniques where cation-anion-cation beds are used. A model that can predict the performance of such a homogeneous bed train will be an important tool in design and operation of water treatment units for ultrapure water, and will complement MBIE programs in use.

Objective

The purpose of this thesis is to develop a model that can predict the breakthrough for a homogeneous bed of resin at very low ionic concentrations. The model for MBIE at very low ionic concentrations developed by Haub and Foutch (1986 a,b) considered the

effect of water dissociation, the ratio of cationic to anionic resin, differing resin exchange rates and differing resin exchange capacities. Temperature effects on resin selectivity coefficients, ionic diffusion coefficients, ionization constant for water and viscosity of bulk solution were also accounted for (Divekar et al., 1987). Capability and complexity of the model were increased through subsequent efforts by Zecchini (1990), Pondugula (1994) and Bulusu (1994). The model is now capable of handling a multicomponent system of ions having arbitrary valences in a mixed bed. This model will be used as a foundation for the current endeavor. The model developed in this thesis will be used to simulate a train of homogeneous beds. Performance of the homogeneous bed train will be compared to that of a mixed bed.

CHAPTER II

LITERATURE REVIEW

A thorough literature review of ion exchange in general, mixed bed ion exchange modeling and homogeneous bed ion exchange modeling (for weak electrolytes) has been performed by Haub (1984), Yoon (1990), Zecchini (1990), Lou (1993) and Chowdiah (1996). This chapter will focus on previous efforts in modeling of homogeneous bed ion exchange at low concentrations (around 10^{-3} M).

Applications of Homogeneous Bed Ion Exchange

Homogeneous bed ion exchange (HBIE) may find use in a wide variety of operations. For example, anion resin in hydroxide form is used to catalyze the reaction of oxygen scavengers such as hydrazine (N_2H_4) and carbohydrazide ($(N_2H_3)_2CO$) with oxygen at ambient temperature (Cutler and Covey, 1995). Golden (1986) lists other uses like color removal from organic solutions, chromatographic separations and 'controlled release.' The concept of 'controlled release' is used to administer macronutrients and trace elements in hydrocultures and to administer drugs at correct levels in medicine.

Homogeneous beds of ion-exchange resins are also used in industry for demineralization of water. Besides homogeneous bed ion exchange, several methods are available for demineralization of water. Design of an ultrapure water facility will be guided by the economics and applicability of these methods with respect to their strengths and weaknesses. Beardsley et al. (1995) compared the following systems for demineralization of water :

1. three bed ion exchange (anion-cation-mixed bed)
2. double pass Reverse Osmosis (RO)
3. RO followed by mixed bed ion exchange

As total dissolved solids (TDS) in feed go up, cost of demineralization increases for all three systems. However, there is a breakpoint below which the ion-exchange system is cheaper. This breakpoint was found to be at 75 ppm of TDS as calcium carbonate in 1987. The breakpoint rose to 130 ppm of TDS as calcium carbonate in the year 1994. Though most waters demineralized in the USA are still above this level, the results of Beardsley et al. (1995) indicate that ion-exchange systems are becoming more economical than RO systems.

Classification of Ion-Exchange Processes and Modeling Approaches

A survey of modeling efforts in ion exchange is incomplete without reference to the classification of ion-exchange processes. As borne out by the following discussion, classification is an integral part of ion-exchange modeling. The assumptions made in

developing the models, their limitations and their applications will also be studied in this survey.

Classification Based on Nature of Interacting Resin and Electrolyte

Ion-exchange processes can be classified on the basis of the nature of interacting resin and the nature of electrolyte. Based on this approach, we can have eight different cases (see Table I). Lou (1993) developed a model capable of handling cases IV and VIII. His model simulated sorption of boric acid at very low inlet concentration, when film diffusion becomes the rate controlling step.

Table I

Classification Based on Nature of Interacting Resin and Electrolyte.

Case Number	Resin Type	Electrolyte Type
I	Strong Base Resin	Strong Acid
II	Strong Base Resin	Weak Acid
III	Weak Base Resin	Strong Acid
IV	Weak Base Resin	Weak Acid
V	Strong Acid Resin	Strong Base
VI	Strong Acid Resin	Weak Base
VII	Weak Acid Resin	Strong Base
VIII	Weak Acid Resin	Weak Base

Classification Based on Rate Determining Step

Typically, the rate-determining step for ion-exchange processes is diffusion of counter ions. The chemical reaction is instantaneous compared with the rate of ionic diffusion. An exception occurs in resins with chelating groups, which form reaction complexes that react very slowly (Helfferich, 1962). The rate determining step also depends on the concentration of the electrolyte in the bulk solution and either particle or film diffusion can be rate determining depending on the solution concentration.

Helfferich (1962) gives the following criterion for identifying the rate determining step :

$$\frac{\bar{Q}D\delta}{CDr_0}(5+2\alpha_B^A) \ll 1 \quad \text{particle diffusion is controlling}$$

$$\frac{\bar{Q}D\delta}{CDr_0}(5+2\alpha_B^A) \gg 1 \quad \text{film diffusion is controlling}$$

$$\frac{\bar{Q}D\delta}{CDr_0}(5+2\alpha_B^A) \approx 1 \quad \text{in the intermediate range, particle as well as film diffusion affect the rate of ion exchange}$$

where,

Q = resin phase concentration of ions

C = bulk phase concentration of ions

D = diffusivity of ions in liquid film

\bar{D} = diffusivity of ions in resin phase

r_0 = radius of the resin bead

δ = film thickness

α_B^A = resin selectivity

The scope of this thesis is limited to ultrapure water applications (ionic concentrations in the range of ppm or less). The above criterion indicates that, controlling mechanism for such applications is film diffusion, because of very low values of ionic concentrations involved.

Classification Based on the Nature of Reaction between Participating Ions and Coions

Helfferich (1965) classified ion-exchange processes involving reactions into four types (see Table II). Helfferich also proposed rate laws for each type of process, under conditions of both film and particle-diffusion control. Blickenstaff et al. (1967a) provided experimental evidence to support Helfferich's model for Type I, under conditions of film-diffusion control. Their study (Blickenstaff et al., 1967b) of Type I, with particle-diffusion controlled neutralization, gave verification of Helfferich's model for this case too, but only under the condition that the concentration of the exchanging electrolyte in the solution phase does not fall with time.

Table II

Classification of Ion-Exchange Processes Involving Reactions

Number	Process Description
I	Counterions from the ion exchanger react with coions from the solution
II	Counterions from the solution react with fixed ionic groups of the ion exchanger
III	Undissociated fixed ionic groups of the ion exchanger react with coions from the solution and form salts that can dissociate into ions
IV	Undissociated fixed ionic groups of the ion exchanger react with counterions from the solution and form new undissociated ionic groups

Mechanism for Ion-Exchange Processes Involving Reactions

The reaction between weak base anion exchanger and acid proceeds via protonation of the ionic sites of the resin by the acid (Helfferich and Hwang, 1985, Bhandari et al., 1992 a,b). Helfferich and Hwang (1985) studied the kinetics of acid sorption by weak base anion exchangers and they assumed that the acid sorption by most weak base resins is irreversible under most conditions. They applied the shrinking core model along with this assumption to describe the above process. However, Bhandari et al. (1992a) hold that neither the shrinking core model nor the assumption of irreversible sorption is valid for most conditions, especially so at lower concentrations than those studied by Helfferich and Hwang (1985) and when the reacting resin has a lower basicity than the ones studied by Helfferich and Hwang (1985). Bhandari et al. (1992a) propose

the existence of a "charged double layer" at the pore walls in the resin. Their reversible sorption model for sorption of strong acids on weak base resins yields a concentration profile in the bead which is similar to the one given by the shrinking core model, but the boundary between reacted shell and unreacted core is diffused.

Bhandari et al. (1992b) extended the "double layer theory" to sorption of weak acids on weak base resins and found that :

1. for weak acids like formic acid, the contribution of undissociated acid to net flux of acid into the resin is higher than the contribution of ionic fluxes, and the rate controlling model of Helfferich and Hwang (1985) is valid only in this case
2. for stronger acids, contribution of ionic flux to net flux of acid into the resin is higher

The "double layer theory" postulates a much weaker Donnan exclusion of coions than that assumed by the rate controlling model. However, Bhandari et al. (1993) found that the results from the "double layer theory" applied to the sorption of dibasic acid on weak base resin agree very well with those from the shrinking core model proposed by Helfferich and Hwang (1985). Bhandari et al. (1993) postulate that, reversibility of sorption is much lower for dibasic acids than monobasic acids. Bhandari et al. (1993) also postulate that, hydrogen coions in a solution of dibasic acid have more access to the resin pores than in the case of monobasic acids. The increased access for hydrogen coions, to resin pores in a solution of dibasic acid, is due to weaker Donnan exclusion in dibasic acids as compared to monobasic acids. A weaker Donnan exclusion of coions in dibasic acids, as compared to monobasic acids, is in turn attributed to stronger sorption of divalent anions by neutralization with two sites in anion resin pores. Thus, both the

“double layer theory” and shrinking core model predict more access for hydrogen cations, to anion resin pores, when bulk solution has polybasic acids. Both models also agree on irreversibility of sorption of polybasic acids on weak base resins.

Models for Homogeneous Bed Ion Exchange at Low Solution Concentrations

All the HBIE models found in the course of this literature survey apply to solution concentrations of 0.001M or more. Kraaijeveld and Wesselingh (1992) studied ion exchange under conditions of film-diffusion control. Their experiments (at solution concentrations of 0.001 M to 0.1 M) show that under conditions of film diffusion control, the ion-exchange processes between sodium - hydrogen and calcium - hydrogen are faster when the hydrogen ion moves from solution to the resin than the case where hydrogen ion moves from resin to solution. They conclude that under the conditions studied by them ion-exchange kinetics depend upon the direction in which exchange is taking place.

Petruzzelli, Liberti et al. (1987) studied binary ion exchange (chloride - sulfate) in the forward and reverse directions and isotopic exchange for sulfate. They concluded that film and particle diffusion both played a role in the exchange kinetics at the concentration range (0.006 M chloride and 0.003 M sulfate) studied by them. The results from their computer simulation combining film and particle diffusion resistance yielded results close to pure film diffusion up to a fractional approach to equilibrium of 0.4. The results were close to pure particle-diffusion control only when complete equilibrium was approached.

Investigation by Liberti, Petruzzelli et al. (1987) into chloride - sulfate exchange at high concentration (0.9 M sulfate, 1.8 M chloride) show that kinetics of ion exchange is particle-diffusion controlled at those concentrations. They also evaluated the results obtained by using Nernst-Planck equations to model the kinetics at high concentration. They found that actual rates at low conversion of the resin were lower than those predicted and the actual rates at high conversion were greater than those predicted. At low conversions, the authors regard retardation by film diffusion as the cause for model inaccuracy and at high conversion, they attribute the inaccuracy to an appreciable change in swelling of the acrylate based resin.

Applicability of Nernst-Planck Equation and Applicability of Complete Donnan

Exclusion at Low Solution Concentrations

The Nernst-Planck equation is a special case of the Maxwell-Stefan equation and the former can be derived from the latter by making assumptions listed in Table III. The Nernst-Planck equation neglects all the terms except the term for friction between the solvent and the ions, and the term for resistance to mass transfer by electrical gradient (Kraaijeveld and Wesselingh, 1992). Kraaijeveld and Wesselingh (1992) modeled the ion-exchange process using Maxwell-Stefan transport equations and used the film thickness as the fitting parameter. Even at the concentration range (0.001 M - 0.1 M) studied by them, the difference in film thickness fitted for Maxwell-Stefan and Nernst-Planck equations was found to be less than three percent. The difference between the

predictions made by Maxwell-Stefan and Nernst-Planck equations is expected to reduce further at the low concentration ranges encountered in ultrapure water applications. Therefore, use of Nernst-Planck equations instead of Maxwell-Stefan equations is justified for work at these concentrations.

Table III

Assumptions for Derivation of Nernst-Planck Equation from Maxwell-Stefan Equation

Assumptions

1. Constant coefficient of diffusion for each ion.
2. All activity coefficients equal unity.
3. No convection (diffusion across a static film).
4. No gradients of temperature and pressure.
5. Electric potential changes only in the radial direction for the resin bead and liquid film.

Complete Donnan exclusion of coions from an ion-exchange resin at low solution concentrations is a well known and widely accepted principal. However, complete Donnan exclusion of coions from the resin does not occur at high solution concentrations and some accumulation of coions is observed in the resin at these conditions (Fernandez et al., 1994). Fernandez et al. (1994) have studied the kinetics and equilibrium of the phenomenon.

Fernandez et al. (1995) have evaluated the pore diffusion model and unreacted core model for chelating ion exchange and cationic exchange under conditions of

reaction control. Helfferich (1984) described a new approach to modeling of multicomponent ion exchange which differs from the usual theoretical approach involving differential material balances and flux equations. The new approach is intended for application to columns with variable feed conditions so as to yield predictions with little calculation effort. The concentration variations along the length of the column are viewed as "waves" and the disturbances created by variations in feed concentrations are compared to interference between waves.

CHAPTER III

Homogeneous Bed Ion Exchange Model

Introduction

This chapter deals with the development of a model for multicomponent, homogeneous bed ion exchange at very low solution concentrations (film diffusion controlling). The mixed bed ion exchange (MBIE) model (Bulusu, 1994) is modified for homogeneous bed ion exchange (HBIE) when either cation or anion exchange resins are used.

There are very few studies of ion-exchange kinetics at very low solution concentrations (less than 10^{-4} M) available in the literature. Experimental as well as modeling efforts in ion exchange have traditionally focused on operations at higher concentrations for homogeneous beds as well as mixed beds. Haub and Foutch (1986a,b) and other workers (mentioned in Chapter I) developed simulation tools for demineralization plants employing mixed bed ion exchange at ultrapure water concentrations and filled the gap. The current model is intended to be an extension of this work into the area of HBIE. Minimization of the computational cost of the

simulation is also of high priority in the current effort. The model development will follow the sequence and nomenclature described by Bulusu (1994).

Assumptions

Table IV lists the assumptions made in this model. These assumptions have been used and justified by earlier workers in MBIE with success. In the course of the literature review (chapter II) new studies were found which have bearing on some of these assumptions and these assumptions will be discussed here. Those assumptions, which have special bearing on HBIE modeling (as opposed to the MBIE models for which these have been justified and tested), will be also discussed.

1. Bulk-Phase Neutralization

Consider a bed of cation-exchange resin followed by a bed of anion-exchange resin. The effluent from the cationic bed has an acidic pH and this effluent is fed to the anionic bed. In the anionic bed, the pH of the solution increases from an acidic pH at the inlet to a basic pH at the exit. Thus, at the inlet the reaction plane for the neutralization reaction will be close to the surface of the resin bead in the liquid film surrounding the bead. The reaction plane will shift away from the resin bead and towards the bulk liquid as the pH increases down the column. Thus, bulk phase neutralization may not be a good assumption for all the conditions encountered in HBIE. However, complexity of the problem increases greatly if liquid-film neutralization is assumed (Haub and Foutch,

1986a). Haub and Foutch (1986a) also conclude that the reaction plane approaches the bulk phase as the ionic concentrations fall to 1×10^{-7} M (at 25 °C). Therefore, a small error is expected due to the assumption of bulk phase neutralization at the concentration levels encountered in ultrapure water applications. In keeping with the objective to minimize model complexity and consequently the computational effort, the assumption of bulk phase neutralization is justified.

2. Liquid-Film Diffusion is Rate Controlling

Resistance from particle diffusion is negligible compared with film diffusion. Haub and Foutch (1986a) first justified and successfully applied this assumption under the conditions of high flow rate and low ionic concentrations encountered in the demineralization plants. Petruzzelli et al. (1987) combined particle and film diffusion in their model for binary exchange of ions. Their results indicate that the solution for combined resistance coincides with that for film diffusion up to 40% conversion of resin at concentration of 0.006 M and particle diffusion becomes important only after 75% fractional approach to equilibrium. Studies by Kataoka et al. (1976) indicate that particle diffusion becomes important only after 80% conversion is reached in the resin at concentration of 0.0025 M. Thus, film diffusion resistance remains the controlling resistance for high conversion of the resin at low solution concentrations.

Table IV

Assumptions Made in the HBIE Model

1. Bulk phase neutralization
2. Liquid-film diffusion is rate controlling
3. Nernst-Planck equation is adequate to model all the interactions between the diffusing ions
4. Pseudo steady state ion exchange
5. Local equilibrium at solid-liquid interface
6. Total Donnan exclusion of coions from the resin beads (no coion flux across the particle surface)
7. No net coion flux in the liquid film
8. No net current flow
9. Electroneutrality is always maintained in the resin, film and bulk liquid
10. Selectivity coefficients are constant throughout the column, and with temperature
11. Binary selectivity coefficients can be applied to multicomponent ion exchange
12. Reaction step is instantaneous when compared to the rate of film diffusion
13. Particle diffusion resistance is negligible
14. Uniform bulk and resin phase compositions
15. Curvature of the liquid film is negligible
16. Activity coefficients are always unity
17. Plug flow, negligible axial dispersion
18. Isothermal, Isobaric operation

Ion-Exchange Equilibria

An ion-exchange resin placed in an electrolyte solution will take up ions from the solution in exchange for counterions from its own ionic groups embedded in the hydrocarbon matrix. After equilibrium is reached, no net exchange of ions is possible between the resin and the solution phases. This equilibrium represents the limit to which demineralization can be achieved with a given ion-exchange resin bed. Consider an ion-exchange reaction,



where,

z_A and z_B are charges on ion A and B

entity with over bar signifies that ion is in resin phase

The law of mass action for this reaction is written as

$$K_A^{B|} = \left(\frac{q_B}{C_B^*} \right)^{z_A} \left(\frac{C_A^*}{q_A} \right)^{z_B} \quad (3-2)$$

where,

$K_A^{B|}$ = resin selectivity for ion A in resin phase replaced by ion B from bulk phase

q_A and q_B are resin phase concentrations of A and B respectively

C_A^* and C_B^* are interfacial concentrations of A and B respectively

The equilibrium constant for the ion-exchange reaction is called the selectivity coefficient. Assumption of local equilibrium at the resin - liquid interface lets us write

the equilibrium relationship in terms of resin phase concentration and interfacial ionic concentrations. The selectivity can be written in terms of equivalent fractions as,

$$K_A^B = \left(\frac{y_B}{x_B} \right)^{z_A} \left(\frac{x_A}{y_A} \right)^{z_B} Q^{(z_A - z_B)} C_T^{*(z_B - z_A)} \quad (3-3)$$

where,

x_A^* and x_B^* are interfacial fractional concentrations of A and B respectively

y_A and y_B are resin-phase fractional concentrations of A and B respectively

C_T^* is total interfacial ionic concentration

Q is total resin-phase ionic concentration (resin capacity)

The interfacial equivalent fraction of an ionic species B can now be written as,

$$x_B^* = y_B (K_A^B)^{-1/z_A} \left(\frac{x_A}{y_A} \right)^{z_B/z_A} \left(\frac{Q}{C_T^*} \right)^{1 - (z_B/z_A)} \quad (3-4)$$

where, we know initial resin loadings y_B and y_A , the resin capacity Q and selectivity coefficient (properties of the resin determined by experiment or known from manufacturer's specification).

If there are a total of n counterions involved in exchange, we can write n-1 such independent equations for equilibria. The material balance at the resin - liquid interface is the nth equation,

$$\sum_{i=1}^n x_i^* - 1 = 0 \quad (3-5)$$

Substitute the n-1 equilibrium equations (for n-1 counterions, of form identical to Equation 3-4) into the material balance (Equation 3-5) to obtain a polynomial in terms of

x_A^* . If the total interfacial concentration C_T^* is known, then the coefficients of the polynomial can be evaluated and the polynomial can be solved to obtain the interfacial equivalent fractions. Refer to Appendix A for a detailed discussion on the methods described here.

The ion-exchange equilibrium is a function of total interfacial concentration which is unknown and must be found from the ionic flux rates (as shown in the following discussion). The flux rates in turn depend on the interfacial and bulk concentrations. Thus, we must start with a guess value for the total interfacial ionic concentration and find the correct value by iterations.

Flux Expressions for Liquid-Film Diffusion

We have assumed that liquid-film diffusion is the rate-controlling step for the ion-exchange process. Therefore, the rate of change of concentration of an ionic species in the resin is same as the rate of diffusion of that species of ion through the liquid film.

Thus,

$$\frac{d\bar{C}_i}{dt} = -J_i a_s \quad (3-6)$$

where,

a_s = surface area of resin beads per unit volume

J_i = flux of ionic species in the liquid film

C_i = resin phase concentration of ions i

Replacing the resin-phase concentration of ions in Equation 3-6 by equivalent fraction of the ions in the resin yields

$$\frac{d y_i}{dt} = - \frac{z_i J_i a_s}{Q} \quad (3-7)$$

In order to find the rate of resin loading, the flux of counterions across the liquid film J_i must be known. J_i is modeled by the Nernst-Planck equation as :

$$J_i = - D_i \left(\frac{\partial C_i}{\partial r} + \frac{C_i z_i F}{RT} \frac{\partial \phi}{\partial r} \right) \quad (3-8)$$

where,

F = Faraday's constant

ϕ = electric potential

R = universal gas constant

r = radial distance

The term for gradient in electrical potential ($d\phi/dr$) in the Nernst-Planck equation is eliminated because the gradient in electrical potential is difficult to evaluate. The gradient in electrical potential is replaced by a function of total equivalent concentration. The flux expressions are then integrated with appropriate boundary conditions to find a relation between the total equivalent concentration C_T and the individual ionic concentration C_i . The method proposed by Franzreb et al. (1993) is used for this purpose. This method yields an exact solution of the flux expression for the special case of counterions with equal valences and yields an approximation for the case of arbitrary counterion valences (Refer Appendix B for a detailed derivation of the methods described

here). The total interfacial concentration of ions (on the resin-liquid interface) is given by,

$$C_T^* = \left[\frac{\sum_{i=1}^n (1 + N_i) D_i x_i^0}{\sum_{i=1}^n (1 + N_i) D_i x_i^*} \right]^{\frac{1}{P+1}} C_T^0 \quad (3-9)$$

where,

N_i = the relative valence for ion i (ratio of valence of ion i to the average value of coion valence) and

P = a parameter in the solution of the flux expression and P is determined by integration of the flux expression between appropriate boundary conditions.

C_T^0 = total bulk-phase concentration of ions

Ionic concentrations within the liquid film are expressed in terms of concentrations at the resin-liquid interface and the bulk concentrations. Ionic flux rates (J_i) for each species of counterions in the liquid film are then given by,

$$J_i = \frac{D_i}{\delta} \left[\left(1 - \frac{N_i}{P} \right) (C_i^* - C_i^0) + N_i \frac{A_i}{z_i} \left(1 + \frac{1}{P} \right) (C_T^* - C_T^0) \right] \quad (3-10)$$

This expression for J_i is valid for any arbitrary number of counterions and coions with arbitrary valences. The film thickness in Equation 3-10 is substituted by

$$\delta = \frac{D_e}{k} \quad (3-11)$$

The effective diffusivity D_e in Equation 3-11 is given by,

$$D_e = \frac{\sum_{i=1}^n |J_i \delta|}{\sum_{i=1}^n |C_i^* - C_i^0|} \quad (3-12)$$

and k is calculated by the correlation of Dwivedi and Upadhyay (1977). The rate at which ions load on the resin is found by substituting value of J_i from Equation 3-10 into Equation 3-7 as described earlier.

Algorithm to Calculate Interfacial Concentrations and Flux Rates As described earlier, the total interfacial concentration must be found by iteration. For this purpose the strategy outlined in Table V is adopted.

Table V

Algorithm for Interfacial Concentrations and Rates of Film Diffusion

1. Assume $C_T^* = C_T^0$
2. Evaluate the coefficients for the polynomial obtained by substituting Equations 3-4 into Equation 3-5
3. Solve the polynomial for x_A^* and calculate x_i^* 's from the equilibrium Equations 3-4
4. Find the value of C_T^* using Equation 3.9.
5. Compare old value of C_T^* with new value. Return to 2 and iterate till C_T^* has converged to a value within the desired tolerance.
6. Calculate the flux rates for ions in the liquid film with Equation 3-10

Material Balance Equation for the Column

In order to predict the effluent concentration with time, a material balance for the column must be setup. A differential material balance can be applied to a very small slice of the resin column. The net increase in the amount of an ionic species present in the slice equals the difference between the influx and efflux of the ionic species. In a film diffusion controlled rate model, the net rate of accumulation (or exhaustion) of an ion in the slice equals the rate of ion transport through the film. The material balance equation for exchange of ions between the resin bed and the solution phase is written as,

$$\frac{u_s}{\epsilon} \frac{\partial C_i}{\partial Z} + \frac{\partial C_i}{\partial t} + \frac{(1-\epsilon)}{\epsilon} \frac{\partial q_i}{\partial t} = 0 \quad (3-13)$$

where,

u_s = superficial fluid velocity of bulk liquid

ϵ = void fraction in the resin bed

Z = bed depth

With dimensionless distance (ξ) and dimensionless time (τ), this equation can be reduced to the following form (refer to Appendix C for definition of dimensionless variables and derivation of the equation)

$$\frac{\partial X_i}{\partial \xi} + \frac{\partial y_i}{\partial \tau} = 0 \quad (3-14)$$

The material balance for the column is integrated using the method of characteristics (Haub, 1984). Appendix D discusses the approach used for solution of the material balance equations and lists the numerical methods applied for the integration.

Calculation of Temperature Dependent Parameters

The HBIE model uses the following temperature sensitive parameters :

1. Viscosity of water. The viscosity of water is estimated at the desired temperature with the relation given in Table VI.
2. Equilibrium Coefficients. Water dissociation equilibrium is a weak function of temperature (see Table VI). The model assumes the ion selectivities are constant with temperature on account of lack of data to compute the temperature effects on this parameter.

Table VI

Water Viscosity and Water Dissociation

water viscosity $\mu = 1.43123 + (T - 273.15)[0.000127065(T - 273.15) - 0.0241537]$

water dissociation $pK_w = \frac{4470.99}{(T)} - 6.0875 + 0.0176T$

3. Diffusion Coefficients The diffusion coefficients and electrical conductivities of ions are interrelated (Helfferich, 1962). If the conductivities (λ_i^0) are available as a function of temperature, diffusion coefficients can be calculated at the desired temperature with the use of Nernst equation,

$$D_i^0 = \left(\frac{RT}{F^2} \right) \lambda_i^0 \quad (3-15)$$

Table VII lists the conductivities as functions of temperature (Divekar et al., 1987). The conductivities estimated by these relationships are used for calculation of diffusion coefficients in this model.

Table VII
Conductance as Function of Temperature

Ion	Conductance
Hydrogen	$\lambda_{\text{H}}^0 = 221.7134 + 5.52964T - 0.014445T^2$
Sodium	$\lambda_{\text{Na}}^0 = 23.00498 + 1.06416T + 0.0033196T^2$
Calcium	$\lambda_{\text{Ca}}^0 = (23.27 + 1.575T)/2.0$
Hydroxide	$\lambda_{\text{OH}}^0 = 1.0474113 + 3.807544T$
Chloride	$\lambda_{\text{Cl}}^0 = 39.6493 + 1.39176T + 0.0033196T^2$
Sulfate	$\lambda_{\text{SO}_4}^0 = (35.76 + 2.079T)/2.0$

Comparison of Material Balance Equations in MBIE and HBIE

So far, the treatment for HBIE modeling has been the same as MBIE with the exception of material balance equations used to describe the column. The material balance used in the MBIE model (Bulusu, 1994) reduces to the following form after applying the dimensionless time and distance variables :

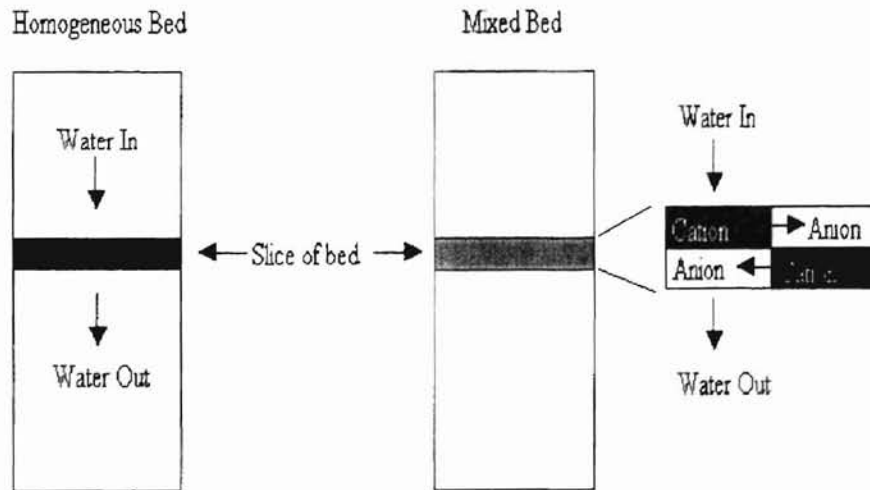
$$\frac{\partial X_i}{\partial \xi_c} + \text{FAR} \frac{\partial y_i}{\partial \tau_c} = 0$$

$$\frac{\partial X_i}{\partial \xi_c} + \text{FCR} \frac{\partial y_i}{\partial \tau_c} = 0$$
(3-16)

The derivatives in Equation 3-16 are with respect to dimensionless variables defined for a common reference ion. In both the models, HBIE as well as MBIE, the column is divided into infinitesimal slices (perpendicular to the column axis) and integration of the column material balance is carried out by finite difference methods. In the HBIE simulation program, effluent from one slice forms the feed for the next slice. A subroutine carries out the algorithm described in Table V for each slice and returns the flux rates to the main program which carries out the task of integrating the column material balance.

Figure 1

Solution Strategies For Differential Material Balance



The solution strategy used in the MBIE model, to solve the column material balance, is different from the solution strategy used in HBIE. The MBIE model further divides each slice into four zones of cationic and anionic resins alternating with one another (see Figure 1). The HBIE strategy does not require this division. In the MBIE model, each zone is treated like a slice of homogeneous resin bed and calculation of flux rates, interfacial concentrations, etc. is carried out for each zone. Thus, effluent from the first zone of cationic resin forms the feed for the next zone of anionic resin and so on. This alternating pattern of homogeneous sub-slices is used to simulate a mixed bed in MBIE.

Simulation of Homogeneous Beds in Series

The HBIE model can be adapted for simulation of homogeneous ion-exchange beds in series. For this purpose, the integration of the column material balance for the second column must be done under the condition of variable feed concentration. The step sizes in time used for integration of column material balances for two columns in series must be equal.

Ion-exchange trains consisting of one cationic-resin bed and one anionic-resin bed in series are simulated and the effect of the order of the beds on the effluent water quality is studied. The performance of a mixed bed unit (predicted by MBIE model) is also compared with the performance of homogeneous beds in series. The procedure used for these simulations is outlined in Appendix E.

CHAPTER IV

HOMOGENEOUS BEDS VS. MIXED BEDS

Abstract

The performance of a mixed bed is compared with that of two homogeneous beds in series for different configurations. Simulations are run for feed water having ionic contaminants at two levels, namely, at concentrations equivalent to city water (several ppm) and at lower concentrations (several ppb). The order of the beds in the homogeneous-bed train is found to affect the effluent pH and the ionic concentration in the effluent.

Introduction

An ultrapure water facility may employ a train of ion-exchange beds consisting of two homogeneous beds followed by a mixed bed (it may also have other units like reverse osmosis included in this train). The order in which the ion-exchange beds are placed in such a train will be decided by feed-water chemistry and the effects of the order of the beds on effluent quality, bed performance and resin life. For instance, consider

feed water contaminated by calcium salts. Calcium hydroxide tends to precipitate on the ion-exchange resin beads at high pH. Therefore, the cation bed must be placed upstream of the anion bed to remove the calcium cations before the water reaches a high pH in the anion bed. If the anion bed is placed upstream for a feed contaminated by calcium, then the calcium ions will precipitate on the resin beads at the high pH encountered in the anion beds. On the other hand, if the cation bed is placed before the anion bed, the cation bed will “slough” off benzene sulfonic acids. These products are formed due to degradation of the cation resin with the passage of time, and can foul the anion-exchange resins in the following bed (Fisher, 1993). If city water is being used as feed, chloride radicals from the city water will decrosslink resins by oxidizing the bonds (Fisher, 1993). In this case, if we have an anion-exchange bed in the lead, then chloride ions can be removed from the feed before they decrosslink resins in subsequent beds.

Thus, feed water chemistry, desired effluent composition, etc., will decide the order in which beds should be placed. Therefore, it is desirable to predict the effect of the order of the beds on effluent quality. How will a mixed bed unit compare with a cationic bed followed by anionic bed or anionic bed followed by cationic bed, if resins in all the beds have the same exchange capacity and resin properties?

Feed Water Conditions, Resin Properties and Bed Parameters

In this chapter, the bed configurations shown in Figure 2 are compared with respect to their effluent quality. The configurations will be referred to by the abbreviations -- ACB for anion bed followed by cation bed, CAB for cation bed followed

by anion bed and MB for mixed bed. Same anion and same cation resin is used in all the configurations. Resin properties are listed in Table IX. The volume of cation resin in all the configurations is same and so is the anion-resin volume. Thus, the total ion-exchange capacity of the anion resin in the ACB, CAB and MB configurations is same. Similarly, total ion-exchange capacity of cation resin in all the configurations is also equal. The bed parameters are listed in Table VIII. Cation-exchange capacity is not equal to anion-exchange capacity in any configuration.

Figure 2

Schematic Diagram of Homogeneous Beds in Series and Mixed Bed

(White for Anion Bed, Black for Cation Bed, Gray for Mixed Bed)

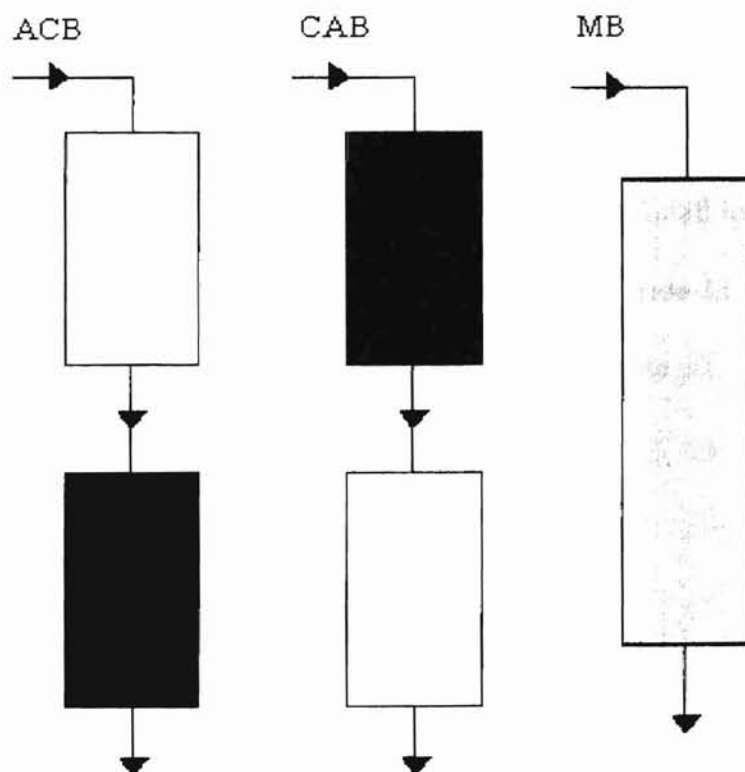


Table VIII

Bed Parameters

	Bed Height	Bed Diameter	Void Fraction
ACB	46.84 cm each bed	152 cm	0.35 in each bed
CAB	46.84 cm each bed	152 cm	0.35 in each bed
MB	93.68 cm (cation/anion volume = 1:1)	152 cm	0.35

Table IX

Resin Properties

	Cation Resin	Anion Resin
	Dowex Monosphere 650C	Dowex Monosphere 550A
Diameter of Resin Bead	0.0625 cm	0.055 cm
Capacity of Resin	1.9	1.1
Initial Resin Loading	1 % for all ions in feed	1% for all ions in feed
Resin Selectivity:	sodium 1.61	chloride 22
	calcium 4.44	sulfate 60

Table X

Feed-Water Condition used in the Simulations

	Case - I	Case - II
sodium	37 ppm	20.24 ppb
calcium	10 ppm	22.4 ppb
chloride	13 ppm	31.24 ppb
sulfate	83 ppm	53.76 ppb
Temperature	25 °C	25 °C
Feed Rate	61x10 ³ cc/s	61x10 ³ cc/s

The performance of different bed configurations is studied at two levels of ionic concentrations, namely, at concentrations equivalent to city water (several ppm) and at lower concentrations (several ppb). The feed water compositions, feed rates and temperatures for both cases are given in Table X.

Results and Discussion

In a mixed-bed ion-exchange column, cations and anions are removed simultaneously and replaced with hydrogen and hydroxide ions, respectively, which then combine to form water. Now consider a homogeneous cation-exchange bed. Here, with progressing cation exchange the hydrogen-ion concentration increases down the bed. Thus, the simultaneous removal of cations and anions in a mixed bed facilitates immediate neutralization and the pH in the mixed bed remains closer to neutral than the

homogeneous bed. In the homogeneous cation bed, pH turns extremely acidic (or basic in an anion bed) down the bed from the inlet to the outlet. Thus, the equilibrium becomes adverse to the ion-exchange process in the homogeneous bed. Consequently, we expect a higher separation efficiency in a mixed bed than a homogeneous bed.

Discussion on Breakthrough Curves

Figure 3 shows sodium breakthrough curves for the case of higher feed concentrations, for all the bed configurations studied. ACB (anion followed by cation bed) gives a sharp breakthrough for sodium, very similar to the MB (mixed bed), while CAB (cation followed by anion bed) gives a comparatively gradual breakthrough. Effluent sodium concentrations before breakthrough are higher for the CAB than the MB and ACB. These differences may be explained by the effect of pH and removal of coions.

Effect of pH. In the ACB configuration, basic effluent of the anion bed is fed to the cation bed. With progressing cation exchange, the pH of the bulk solution in the cation bed of ACB turns increasingly acidic. In the mixed bed, the simultaneous removal of cations and anions facilitates immediate neutralization and the pH in the mixed bed remains closer to neutral than the homogeneous bed. Thus, the pH of the bulk solution in the mixed bed is close to neutral and it changes from basic to acidic in the cation bed of the ACB configuration. These pH conditions are more favorable for cation exchange than the pH in the lead cation-resin bed of the CAB configuration, where the feed is

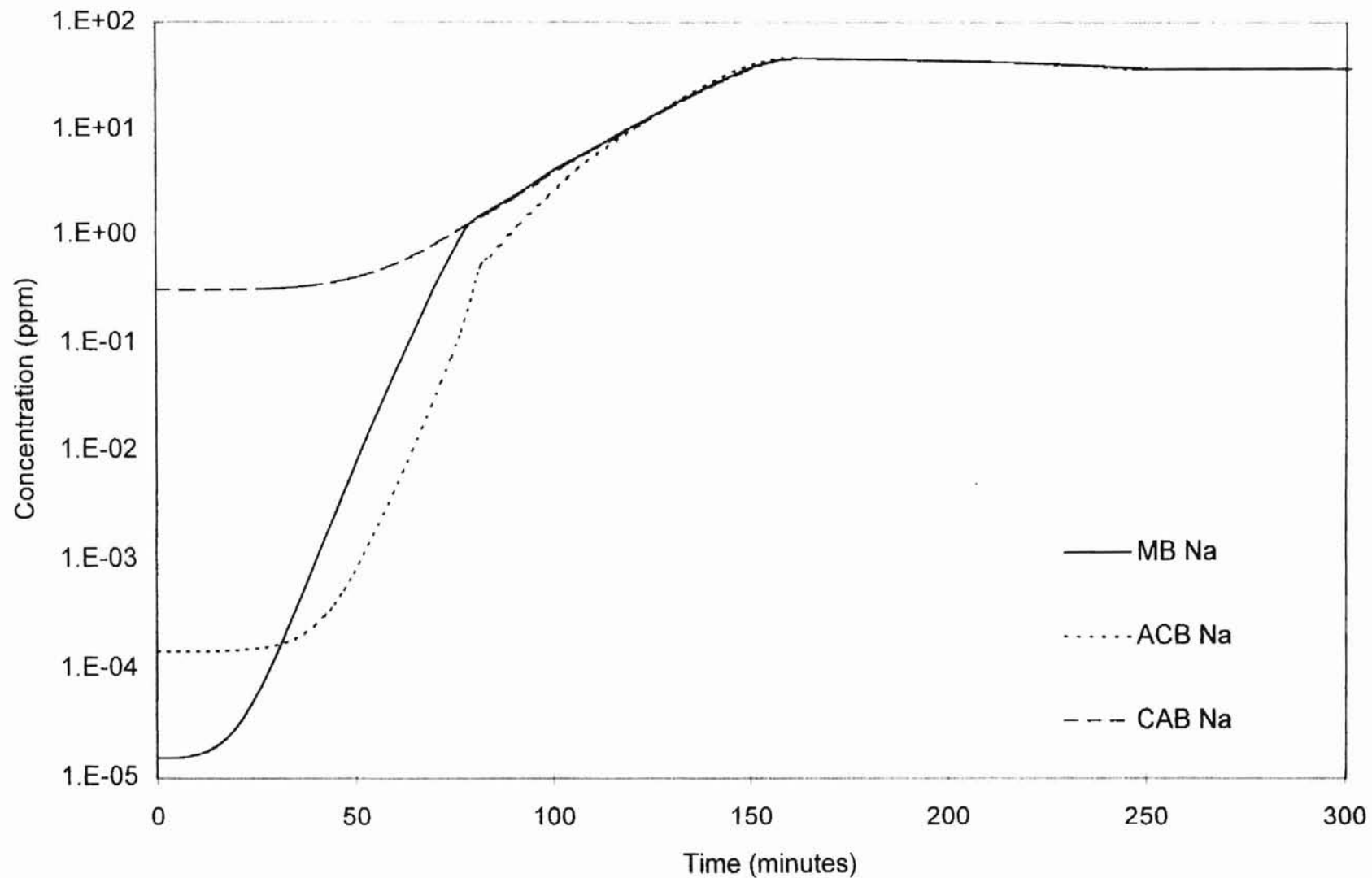


Figure 3. Sodium Breakthrough for ACB, CAB and MB (high concentrations)

neutral and turns acidic from inlet to outlet with progressing cation exchange. An acidic pH in the lead cation bed of CAB results in an unfavorable equilibrium for cation exchange. Consequently, the effluent cation concentration before breakthrough is higher than ACB and MB.

Removal of coions. The anion concentration is constant with time for any fixed point in the cation bed of CAB, while in the other two cases, i.e., MB and ACB the anion concentration is changing with time at any given distance in the bed. However, the effect of coion removal¹ is expected to be very weak (Franzreb, 1993).

Figure 4 shows calcium breakthrough for ACB, CAB and MB for higher feed concentration. The calcium leakage for CAB again stands apart from the ACB and MB, but the differences are less pronounced for calcium as compared to those for sodium (Figure 3). The difference in performance of CAB as compared to ACB and MB may be attributed to an unfavorable pH (unfavorable equilibrium) and the effect of coion removal as in the case of sodium.

¹ This effect of coion concentration, on the rate of ion exchange, is incorporated in the model through the use of Franzreb's (1993) method to solve the Nernst-Planck equation for the ionic flux in the static film assumed to exist around a resin bead. This method uses the coion concentrations to find the mean value of the coion valences. The mean coion valence is used to find the relative valence of the counterions for the solution of the Nernst-Planck equation.

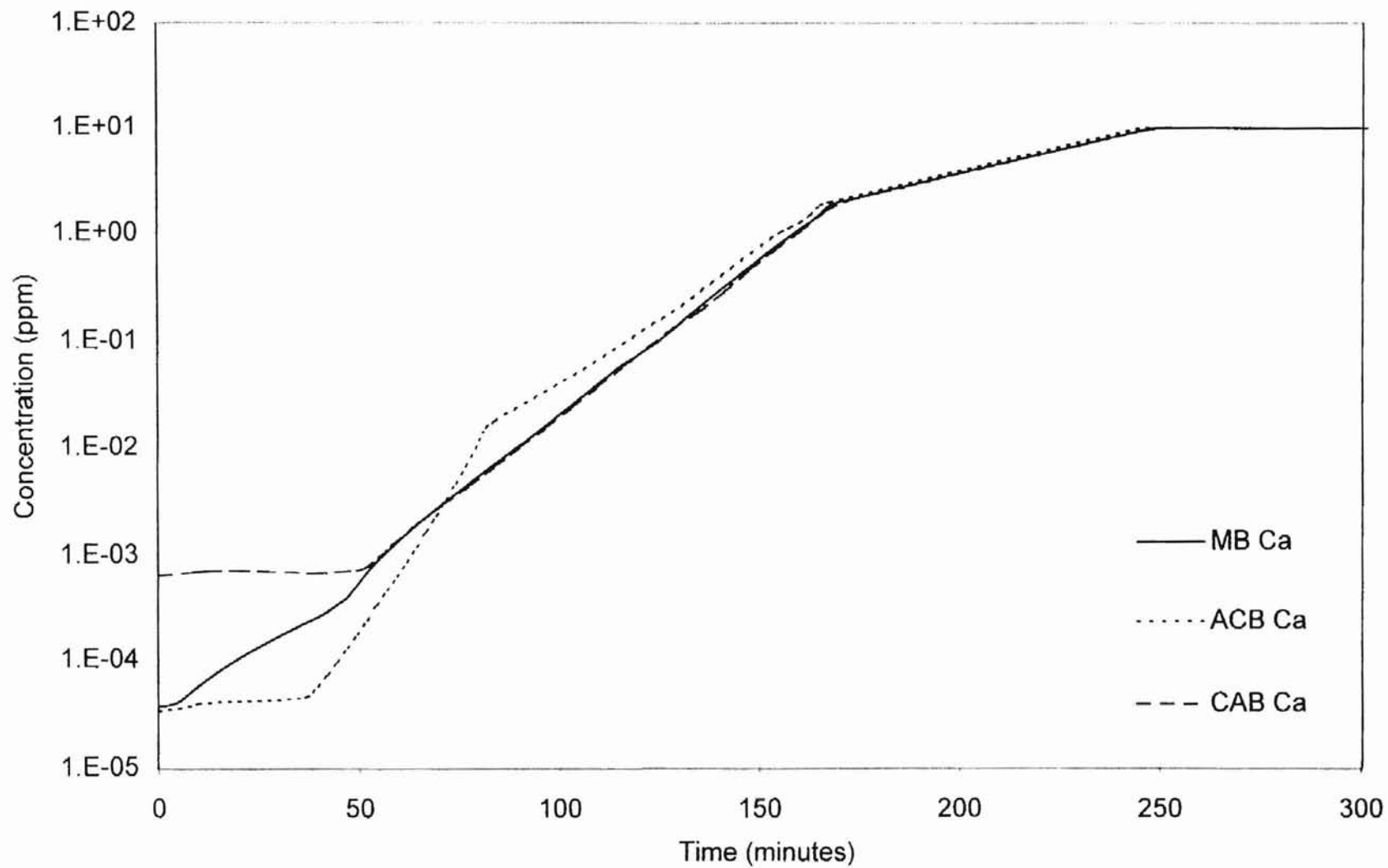


Figure 4. Calcium Breakthrough for ACB, CAB and MB (high concentrations)

The discontinuities in the breakthrough curves (Figure 3 and Figure 4) are ascribed to the following factors:

Change in the Cation being Replaced from the Cation Bed. Sodium breakthrough for ACB, CAB and MB occurs between 10 and 50 days (Figure 3). The sodium breakthrough signifies that all hydrogen in the cation bed has been exhausted. Coincident with the sodium breakthrough, effluent calcium concentration also rises sharply for all the configurations because the calcium now begins to replace sodium in the bed instead of hydrogen. Sodium has higher selectivity than hydrogen, which makes the former more difficult to replace than hydrogen.

Log-scale on the Y-axis of the plot. The concentrations in the figures are plotted on logarithmic scale. This magnifies small changes in the effluent concentration. These small changes in effluent concentrations may occur on account of :

1. changes in feed pH and coion concentrations (when the cation bed is downstream of anion bed -- ACB configuration),
2. instability in the numerical integration.

Figure 5 shows that, even at lower concentrations (several ppb), sodium leakage from the CAB is higher than ACB and MB. Calcium leakage (Figure 6), however, does not show pronounced differences for different configurations, at lower concentrations. These differences between the breakthrough curves for different configurations at higher concentrations (Figures 3 and 4) were explained on the basis of effect of pH and removal

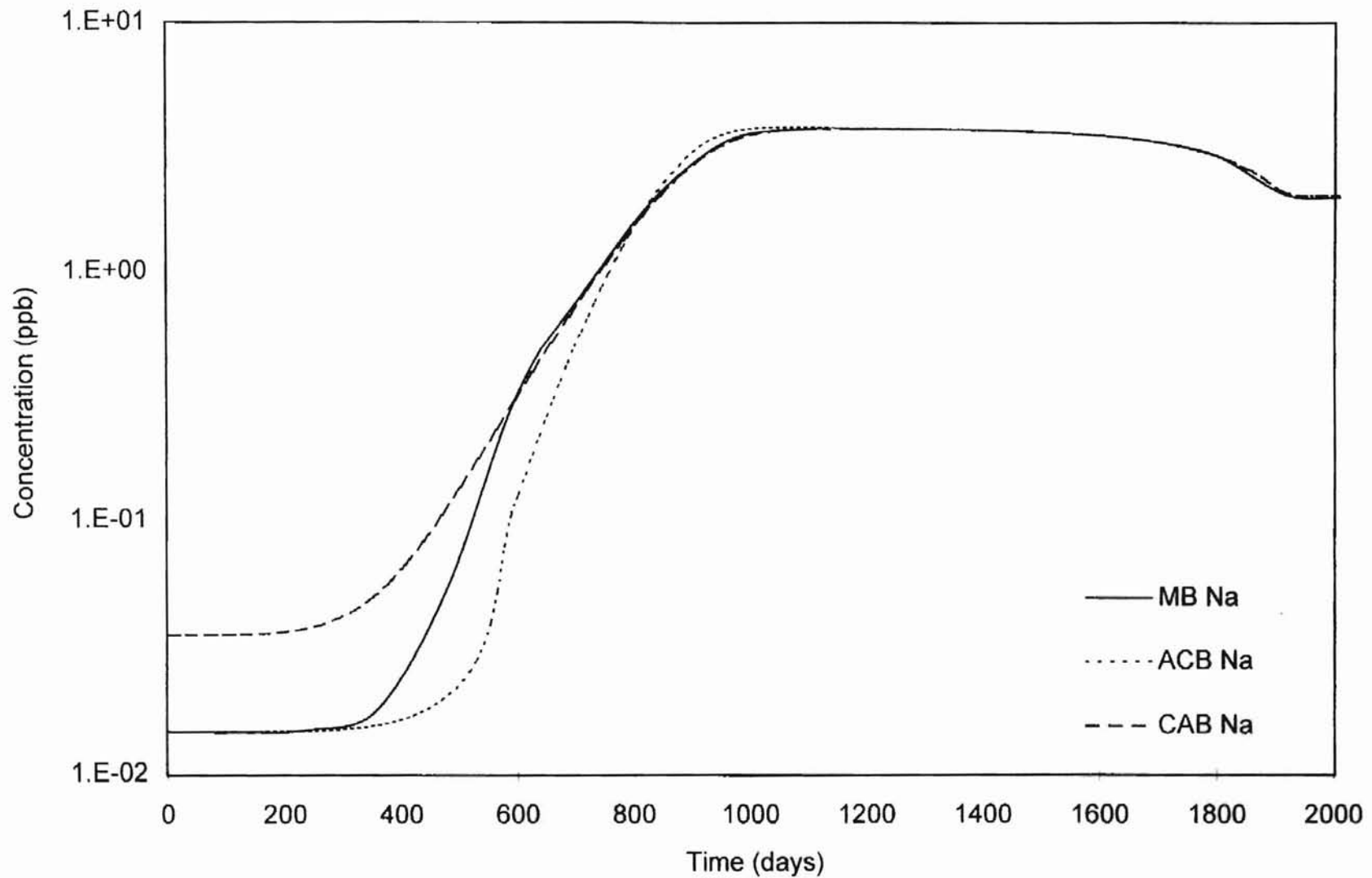


Figure 5. Sodium Breakthrough for ACB, CAB and MB (low concentrations)

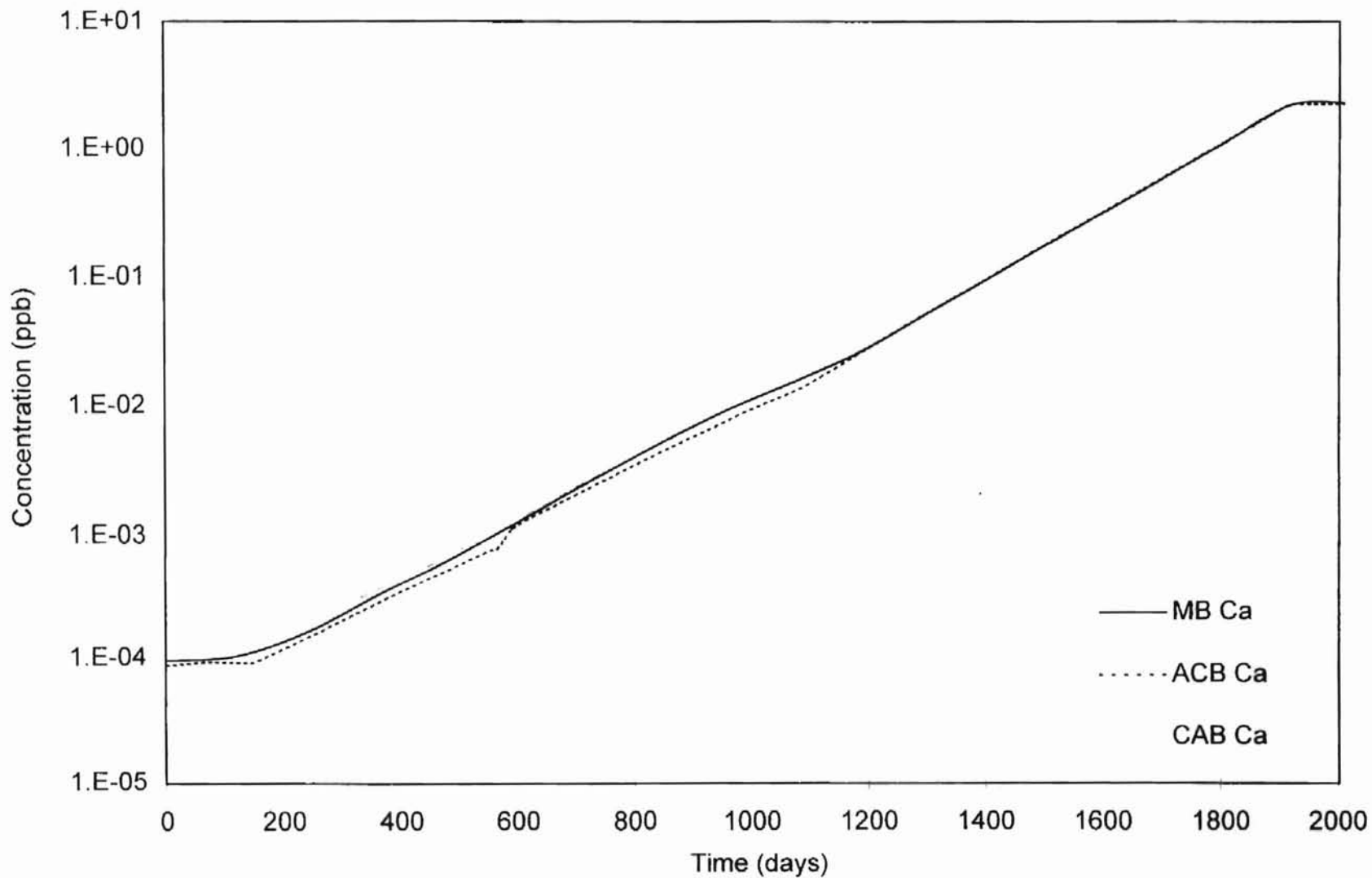


Figure 6. Calcium Breakthrough for ACB, CAB and MB (low concentrations)

of coions. At lower concentrations, these factors are expected to have a smaller effect because the magnitude of changes (in pH as well as coion concentrations) is smaller at lower concentrations. Moreover, coion removal is expected to have a smaller effect, as the concentrations approach the ideal case of infinite dilution (at infinite dilution, the coions will have no effect at all on the exchange of counterions).

The initial leakage of chloride anions for different configurations is shown in Figure 7 for the case of higher feed concentrations. In this case, the ACB configuration is seen to have the highest chloride leakage before breakthrough. MB gives the least chloride leakage, while CAB gives an initial chloride leakage intermediate to ACB and MB. The high leakage of chloride from ACB can be explained in a manner similar to the higher leakage of sodium from CAB, that is, on the basis of the pH and the effect of coion removal.

Effect of pH. The pH conditions in the mixed bed and in the anion bed of the CAB configuration are more favorable than the pH in the lead anion resin bed in the ACB configuration for anion exchange. An adverse pH (basic) in the lead anion bed of ACB results in an unfavorable equilibrium and consequently a higher effluent anion concentration before breakthrough.

Removal of coions. The cation (coion) concentration is constant with time for any fixed point in the anion bed of ACB, while in the other two cases, i.e., MB and CAB the cation (coion) concentration is changing with time at any given distance in the bed. As stated earlier, the effect of coion removal is expected to be very weak (Franzreb, 1993).

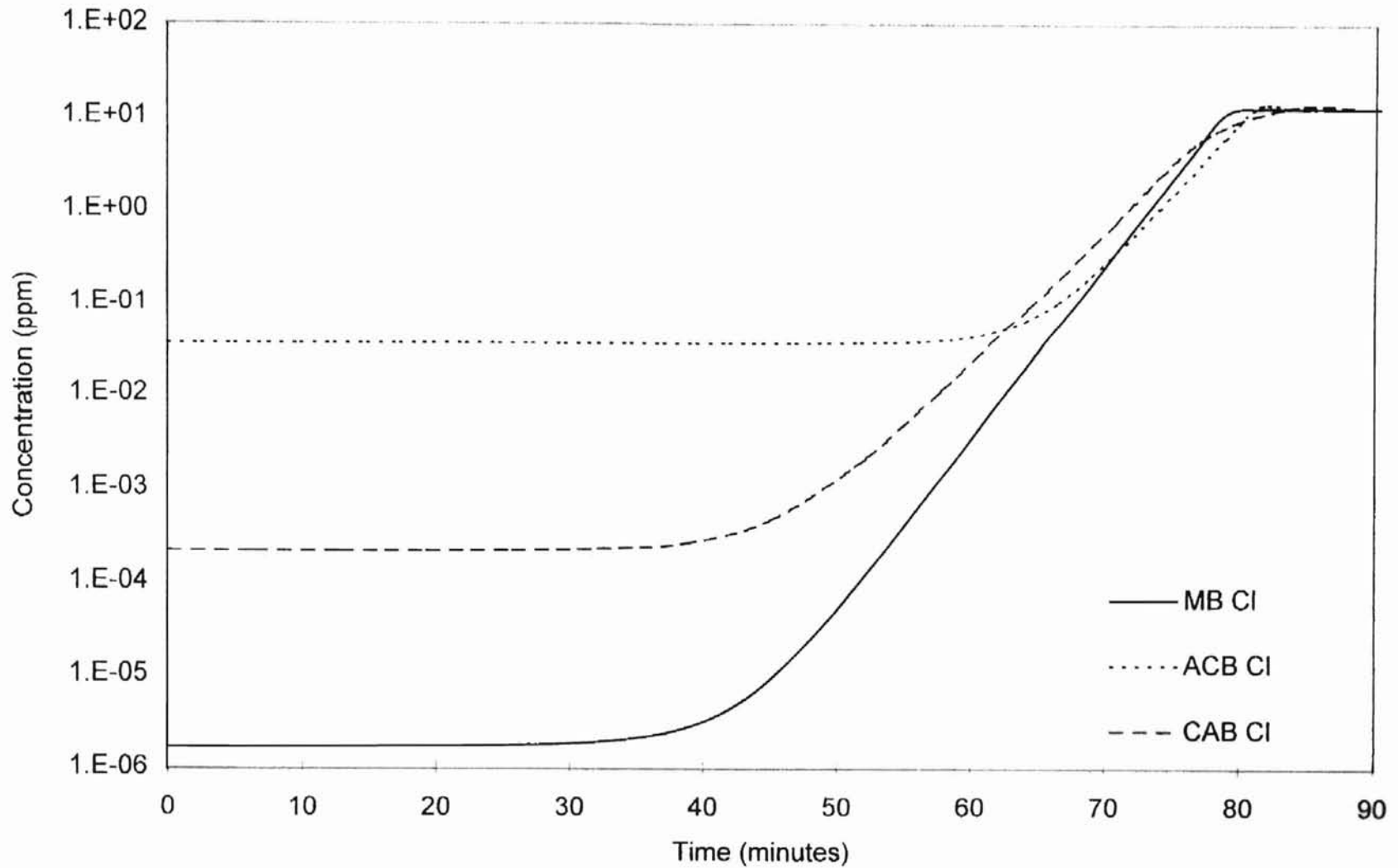


Figure 7. Chloride Breakthrough for ACB, CAB and MB (high concentrations)

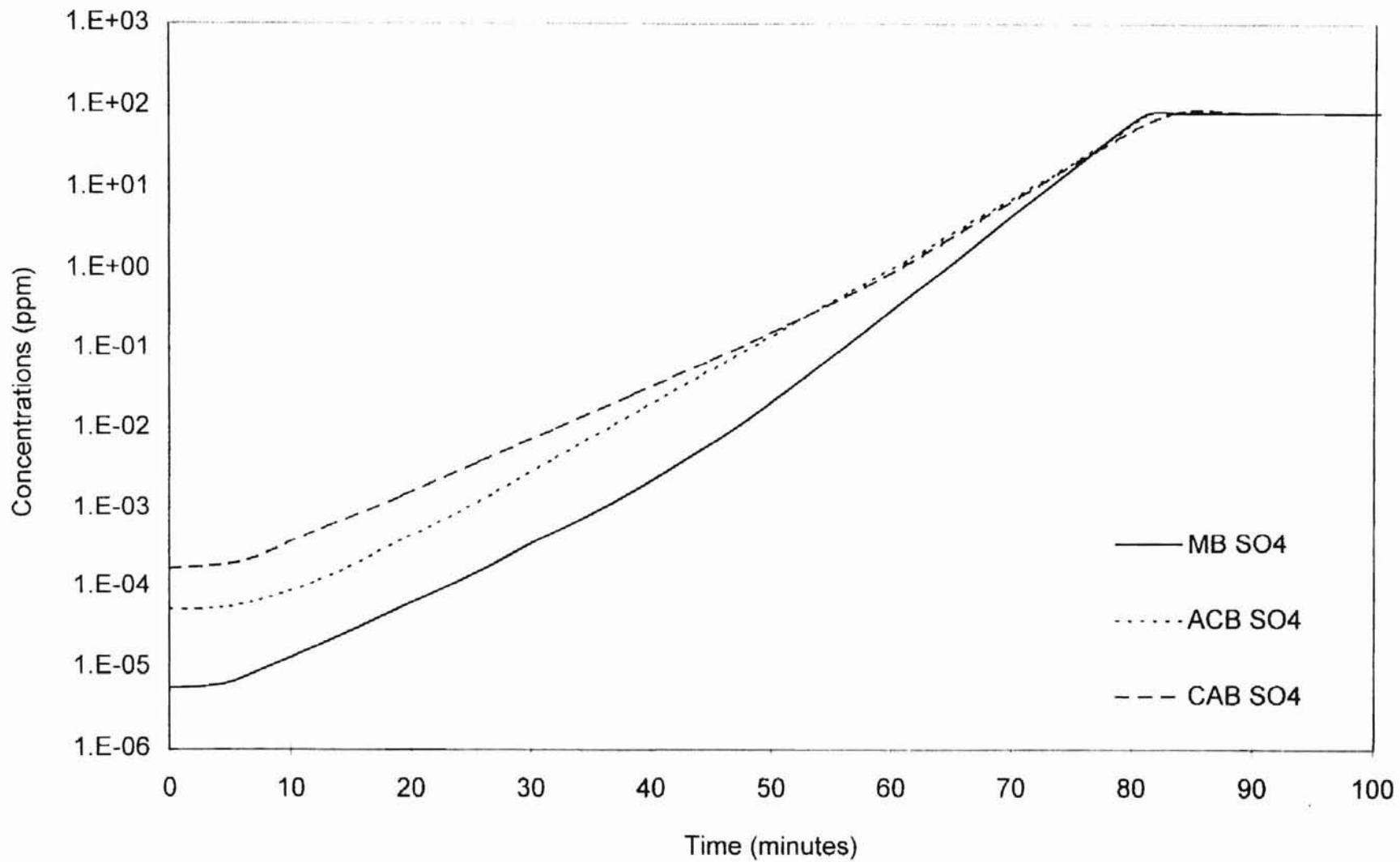


Figure 8. Sulfate Breakthrough for ACB, CAB and MB (high concentrations)

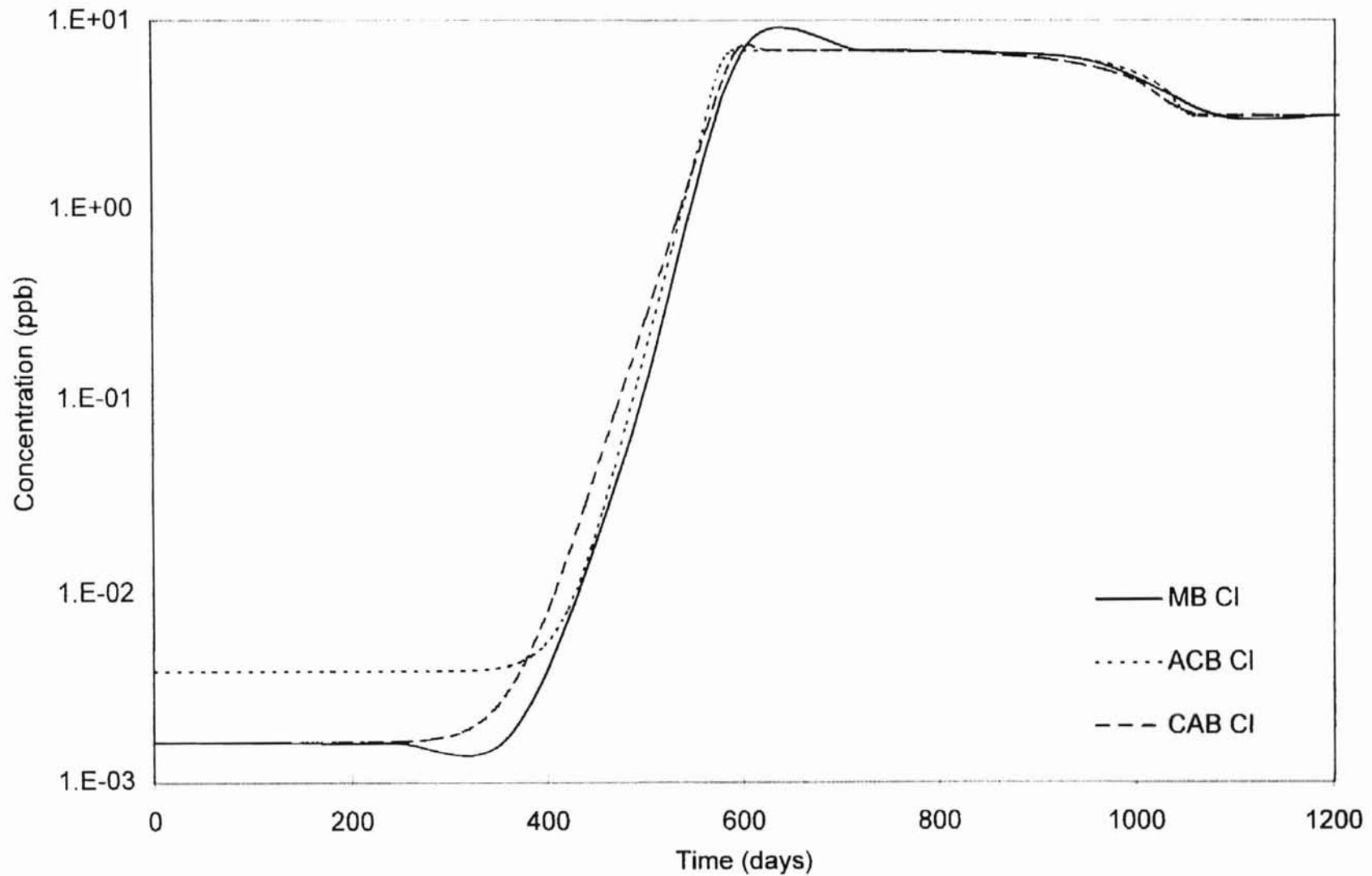


Figure 9. Chloride Breakthrough for ACB, CAB and MB (low concentration)

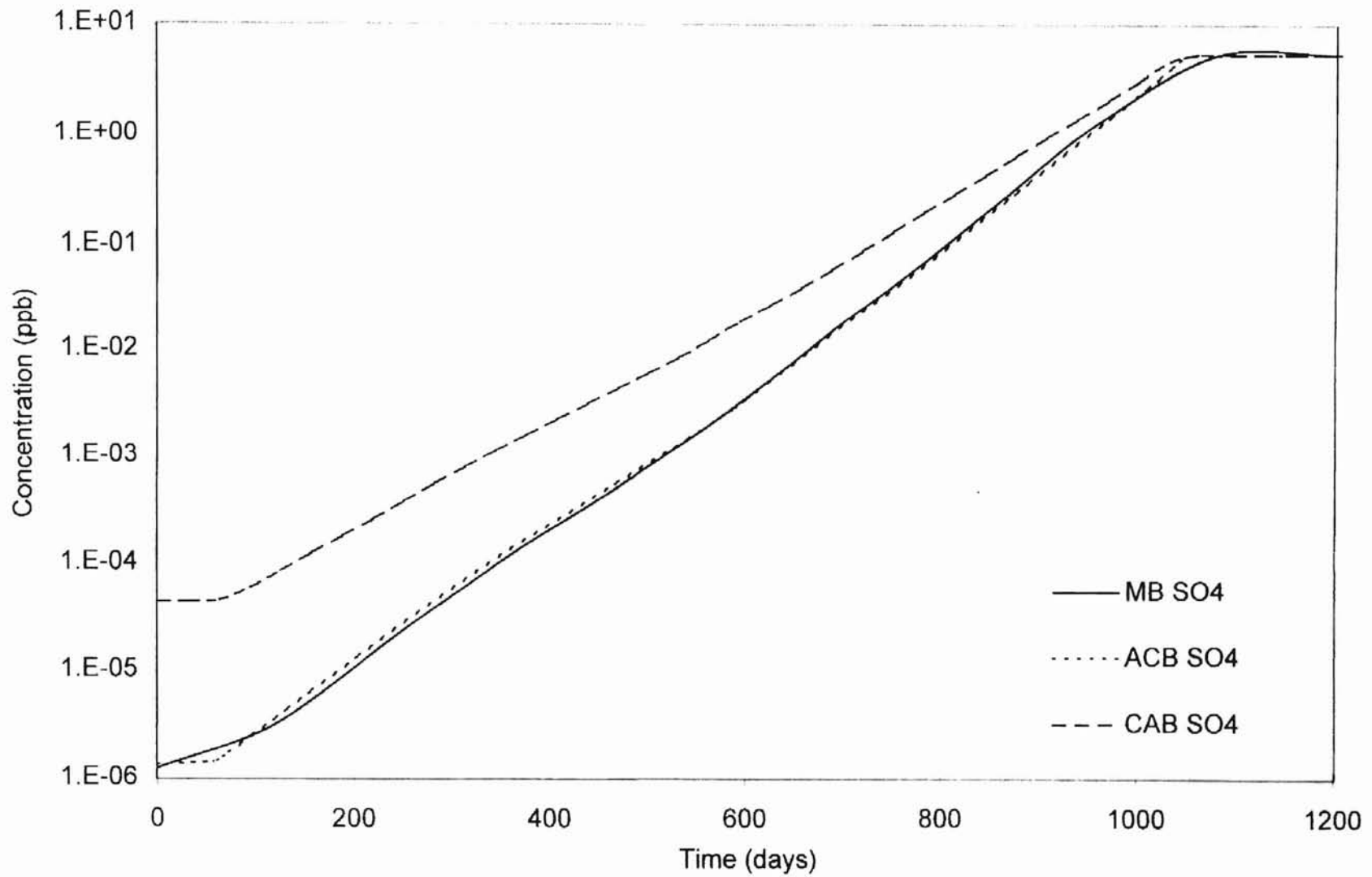


Figure 10. Sulfate Breakthrough for ACB, CAB and MB (low concentrations)

Figure 9 shows the history of chloride concentration in the effluents for the three configurations for lower feed concentrations. At lower concentrations (several ppb) also, chloride leakage from the ACB is higher than CAB and MB. A small dip is seen between 200 days and 400 days in the chloride throw from MB. This dip is attributed to instability in the numerical integration of the column material balance.

The sulfate leakages from the beds (for higher feed concentration) are shown in Figure 8. Sulfate leakage from ACB is not higher than sulfate leakage from CAB, as one would expect after studying chloride leakages. MB gives the lowest sulfate leakage of all three configurations. The same observations are valid for sulfate leakages at lower feed concentrations (Figure 10), namely, sulfate leakage from ACB is not higher than sulfate leakage from CAB and, MB gives the lowest sulfate leakage of all three configurations. This difference between chloride and sulfate leakages may be due to the binary charge on the sulfate ion (as opposed to the unit charge on the chloride radical). Consequently, the effect of feed pH on the sulfate breakthrough is not similar to the effect of feed pH on chloride breakthrough.

The question now is: How can the effect of feed pH on monovalent-ion breakthrough be different from the effect of feed pH on divalent-ion breakthrough? The answer to this question may lie in the effect of the feed pH on the mass-transfer coefficients of the counterions. The mass-transfer coefficient of the counterions is a weak function of the bulk-phase pH. The feed pH may have different effects on mass-transfer rates of monovalent and divalent ions and may thus affect their breakthrough.

Leakages of calcium from MB and ACB are lower than those from CAB (figures 4 and 6). The calcium breakthrough curves are similar to those of sodium though the

calcium is a divalent cation while sodium is monovalent. Thus, feed pH does not seem affect the calcium breakthrough (and mass-transfer coefficient) to the same extent as it affects the sulfate breakthrough.

Discussion on pH of Effluents

Figures 11 to 16 show pH histories of the effluents for different configurations at high and low feed concentration levels studied here. The pH of the effluent from different configurations shows roughly similar trends at low as well as high feed concentrations, with the difference that, the magnitude of changes in effluent pH (with time) is smaller at lower feed concentrations for all configurations.

As seen in Figure 11, the pH of effluent from MB is close to neutral for a neutral feed, before breakthrough is reached. The effluent pH is acidic for the ACB and basic for the CAB, before any breakthrough is reached. Thus, for ACB or CAB, before either cation or anion breakthrough is reached, the effluent pH depends on which bed is placed at the end of the ion-exchange train.

A comparison of breakthrough curves for cations and anions at higher feed concentrations (Figure 4 and Figure 8) shows that the anion resin reaches saturation at approximately 80 minutes while cation resin reaches saturation at 250 minutes. Thus, anion resin reaches saturation before the cation resin. This leads to a fall in effluent pH for all the configurations (Figure 11) after the anion breakthrough has started at around 55 minutes. At 80 minutes, anion resin has reached saturation and effluent pH is at a minimum, because the anion resin no longer exchanges anions while the cation resin

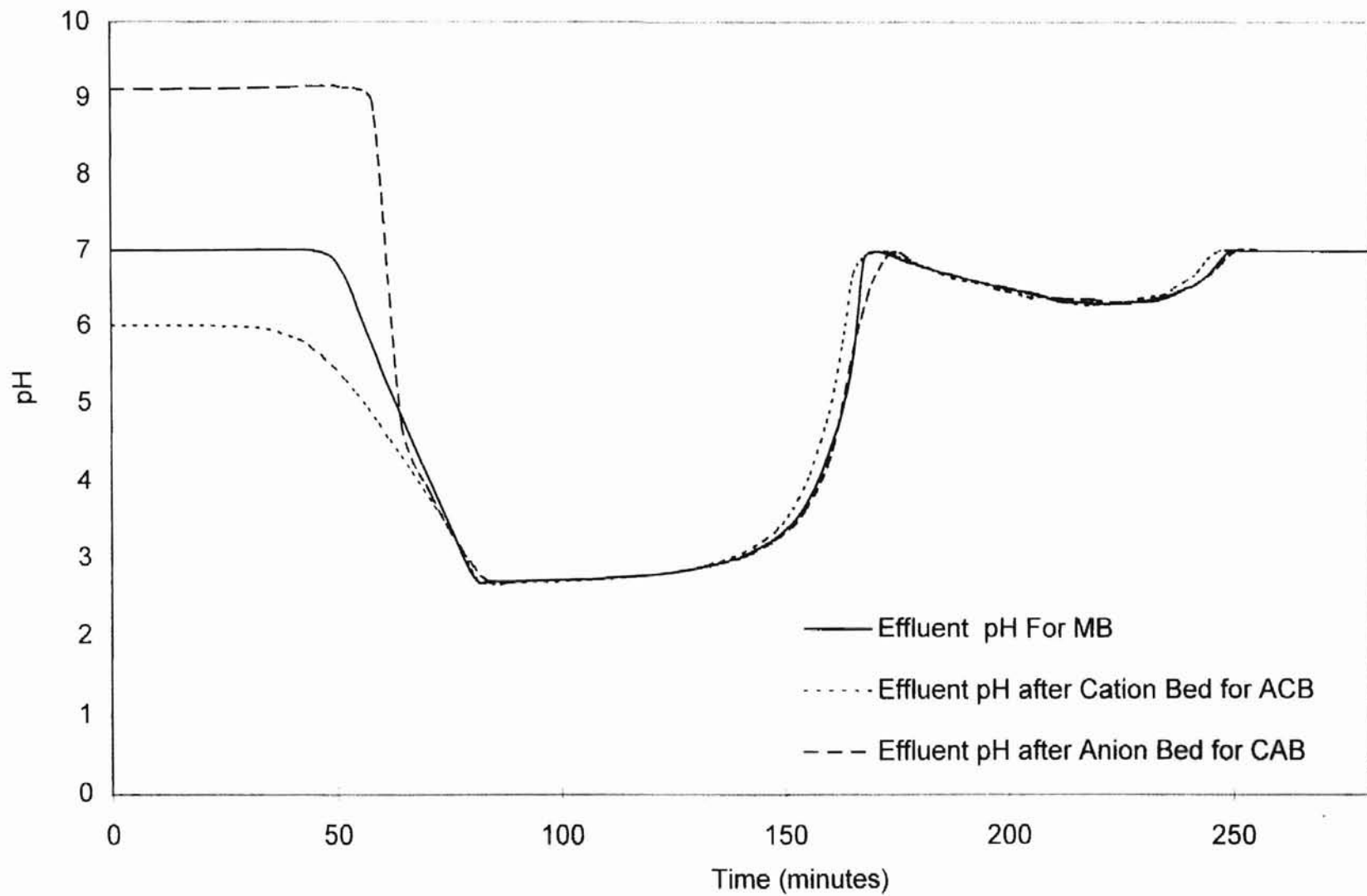


Figure 11. pH of Effluent for ACB, CAB and MB (high concentrations)

continues to replace cations in the solution with hydrogen ions leading to an acidic effluent. As the cation breakthrough occurs, the effluent pH rises and reaches a peak (around 170 minutes). This peak can be attributed to sodium throw from the cation bed as follows:

The effluent pH, is a function of the charge balance in the bulk solution. If the cation concentration (sodium plus calcium) is greater than the anion concentration (chloride and sulfate), effluent pH will be basic. Thus, a rise in cation concentration (sodium plus calcium) results in a rise in effluent pH.

As the throw of sodium decreases, the charge balance favors a lower pH and the effluent pH falls again. At approximately 250 minutes, the cation bed is saturated with calcium (Figure 4) and the effluent pH reaches the same value as the feed pH.

Figure 12 and 13 show the history of effluent pH for the ACB and CAB configurations respectively. The intermediate stream between two beds of an ion-exchange train is shown as a broken line, while the final effluent from the train is shown as an unbroken line in both figures.

Refer to Figure 12 for the following discussion. The anion-bed effluent has a very high pH till the anion-exchange bed is replacing anions with hydroxide ions. But, once the anion bed reaches saturation (at 80 minutes), the effluent from anion bed is same as the feed to the anion bed. Thus, in Figure 13 also, after 80 minutes, the effluent from CAB is same as the effluent from the cation bed (the first bed in the CAB train). Compare Figure 13 with Figure 12. We observe a fall in the pH of the effluent from ACB as well as CAB after the anion bed gets saturated. The history of effluent pH from the ACB, CAB and MB are same after this point. As the cation breakthrough occurs, the

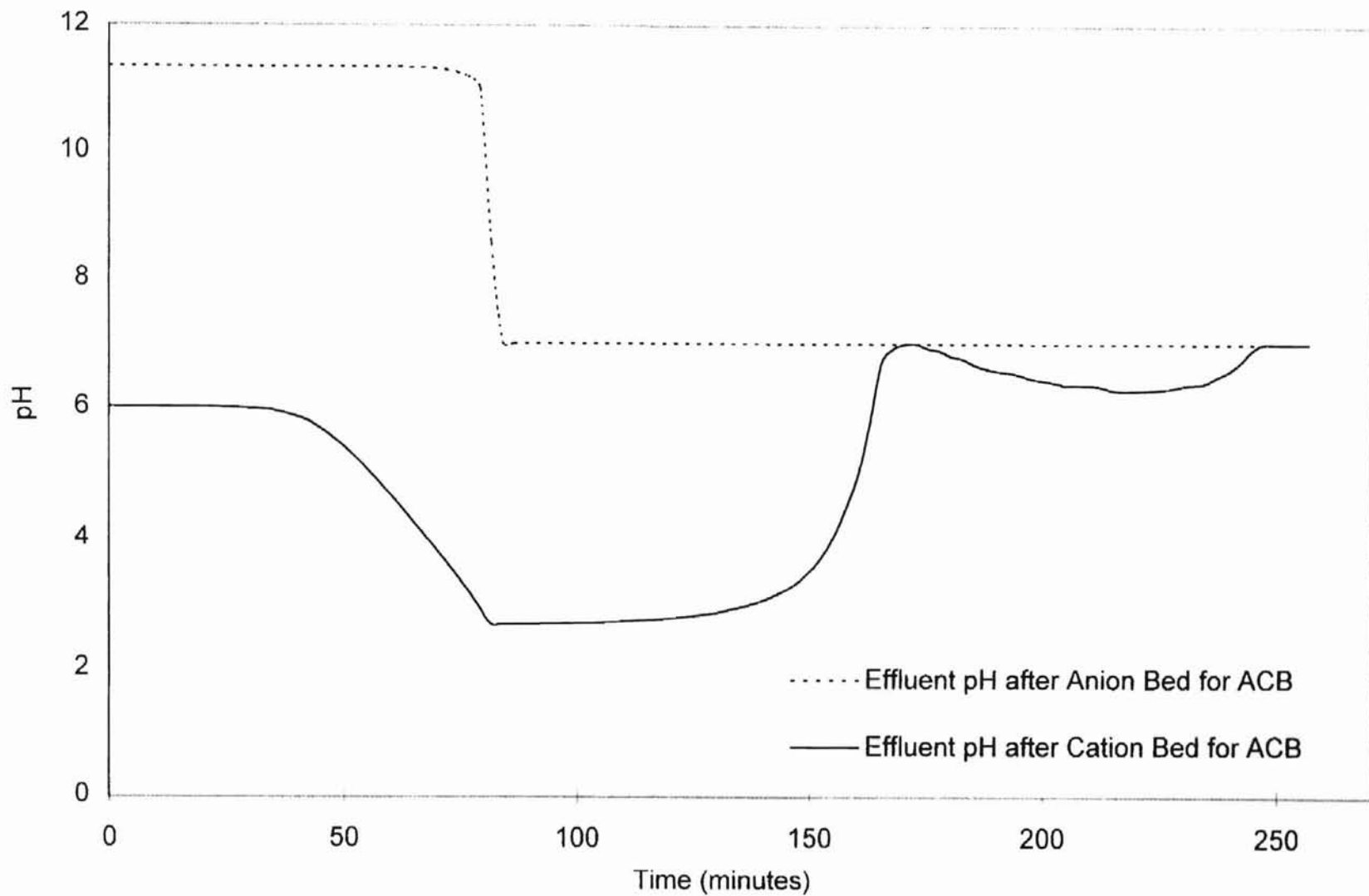


Figure 12. pH History for ACB (high concentrations)

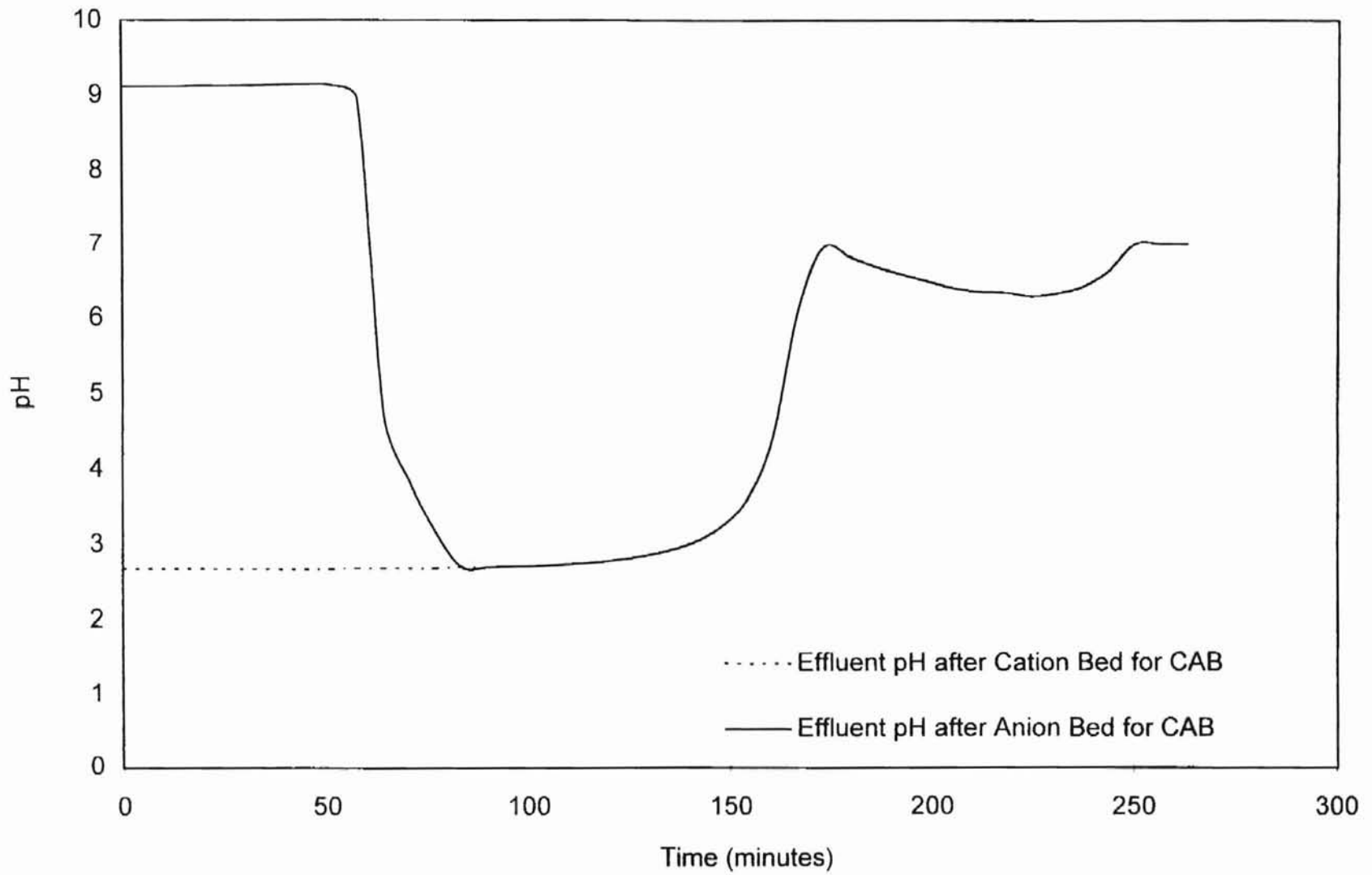


Figure 13. pH History for CAB (high concentrations)

effluent pH rises and reaches a peak (around 170 minutes). This peak can be attributed, to sodium throw from the cation bed, as follows:

The effluent pH, is a function of the charge balance in the bulk solution. If the cation concentration (sodium plus calcium) is greater than the anion concentration (chloride and sulfate), effluent pH will be basic. Thus, a rise in cation concentration (sodium plus calcium) results in a rise in effluent pH.

As the throw of sodium decreases, the charge balance favors a lower pH and the effluent pH falls again. At approximately 250 minutes, the cation bed is saturated with calcium (Figure 4) and the effluent pH reaches the same value as the feed pH.

Refer to Figure 14 for the pH history of effluents from ACB, CAB and MB at lower feed concentrations. The pH changes involved in this case are smaller than those at higher feed concentrations. Also, for very low feed concentrations, the differences in effluent pH between ACB, CAB and MB are less prominent than at higher feed concentrations. As seen in Figure 14, the pH of effluents from ACB, CAB and MB are close to neutral for a neutral feed, before breakthrough is reached. The effluent pH, is a function of the charge balance in the bulk solution. Therefore, at about 400 days, the pH of the effluent from all the configurations begins to fall as the anion beds approach saturation and anion breakthrough begins. This trend continues up to 600 days of column operation and the pH of the effluents reaches a minimum value of 6.63 (approximately) at 600 days. The effluent pH begins to rise after 600 days due to cation breakthrough and sodium throw from the cation bed. At 1000 days of column operation, the throw of sodium from Cation bed reaches a peak and stabilizes at that value till 1600 days. This results in a constant pH of the effluent during this period (1000 days to 1600 days). After

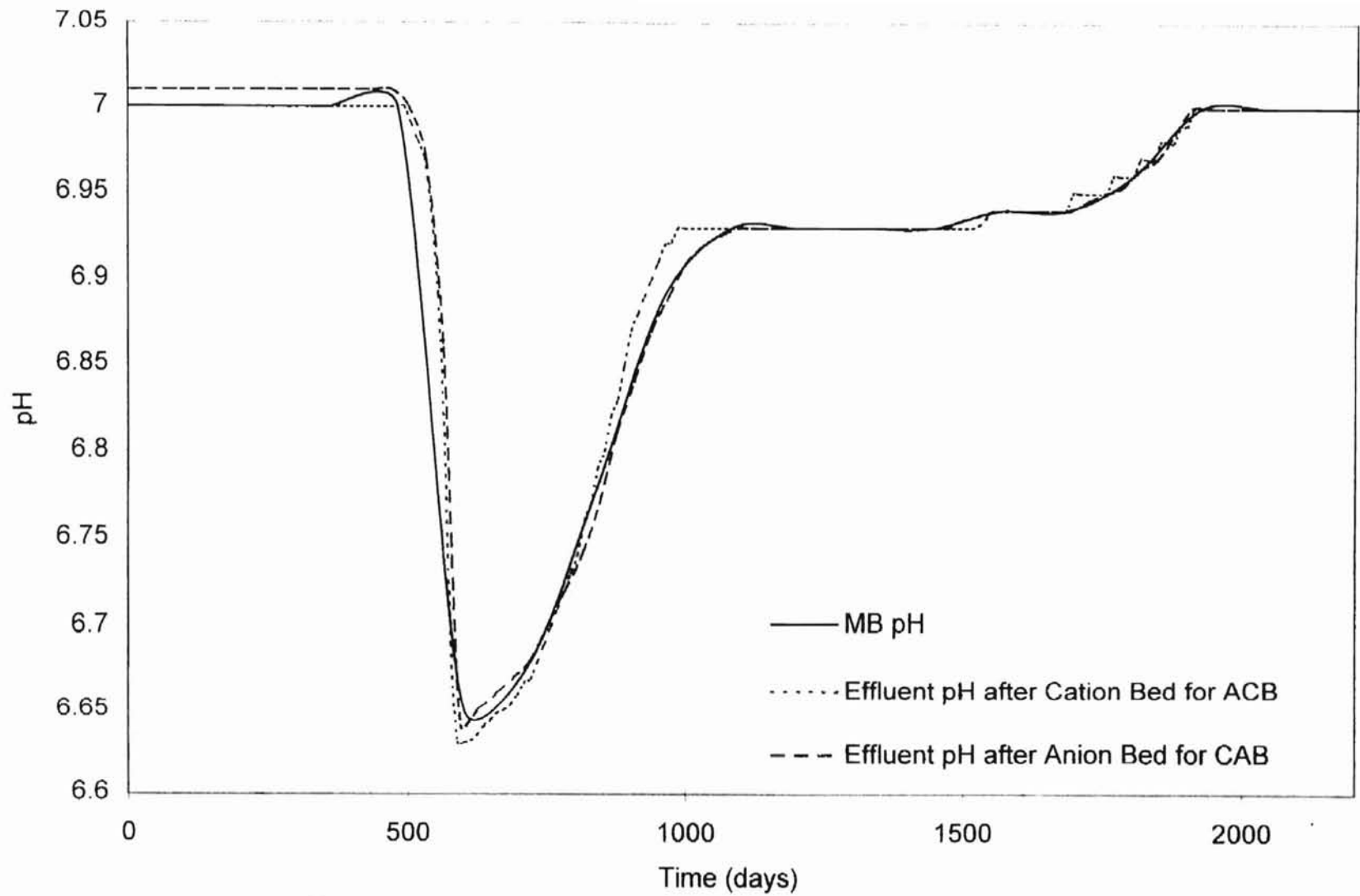


Figure 14. pH of Effluent for ACB, CAB and MB (low concentrations)

the sodium throw from Cation bed falls to feed concentrations, the Cation bed can be said to be saturated with calcium and the effluent pH rises as calcium concentration in the effluent rises to feed concentration of calcium. At 2000 days the effluent pH is same as feed pH because both beds are now saturated.

Figure 15 and Figure 16 show the history of effluent pH for the ACB and CAB configurations respectively. The intermediate stream between two beds of an ion-exchange train is shown as a broken line, while the final effluent from the train is shown as an unbroken line in both figures. The anion breakthrough (Figure 15) begins first as seen from the drop in pH of the anion-bed effluent after 400 days of operation. Comparison of Figure 9 with Figure 15 reveals that the throw of chloride ions from anion bed stabilizes at 600 days to a peak value. This leads to a stable effluent pH (for anion bed, seen as broken line) from 600 days till the chloride throw stops (anion bed saturated with sulfate) at 1000 days and the effluent pH falls again to stabilize at feed pH. The anion bed is saturated with sulfate (at 1000 days) before the cation bed is saturated with calcium (at approximately 2000 days). Comparison of Figure 16 with Figure 9 similarly reveals that anion breakthrough begins at 400 days and this leads to a drop in pH of the CAB effluent till it reaches a minimum at 600 days. Thereafter, it follows the same curve as the pH of effluent from the cation bed. We observe that the pH histories of effluents from ACB, CAB and MB follow identical paths after this point (600 days) and have identical interpretation (given in discussion on Figure 14).

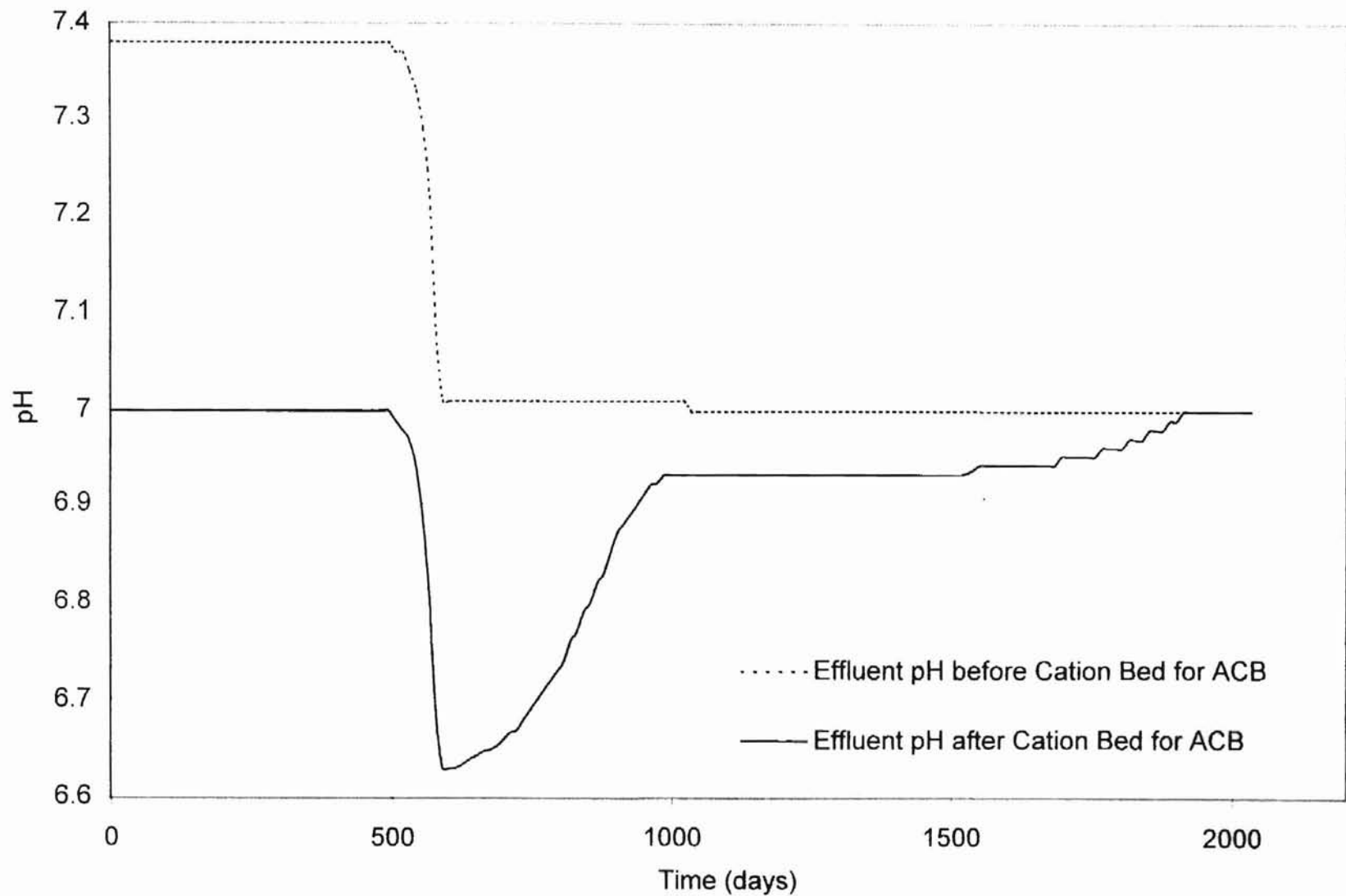


Figure 15. pH History for ACB (low concentrations)

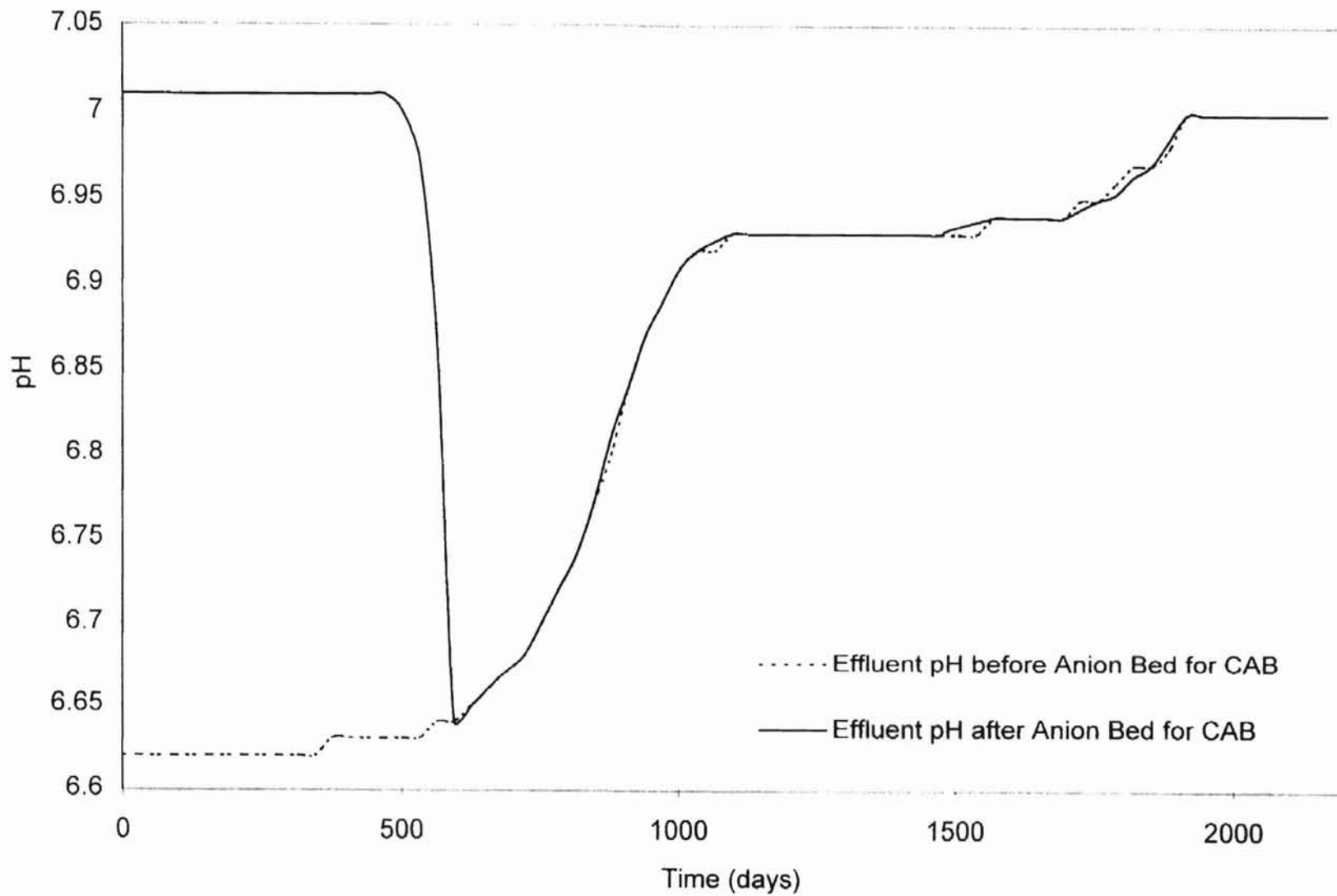


Figure 16. pH History for CAB (low concentrations)

The step changes in pH at low feed concentrations are attributed to the following :

1. increased resolution of changes in concentration (of Hydrogen ion) when these changes are viewed on the log-scale (pH is negative logarithm of Hydrogen ion concentration to base 10).
2. changes in pH get further magnified because a small range of pH values is stretched over a large area in the Y direction (in other words, the minimum and maximum pH values on the Y axis differ by only 0.45 or 0.8).

Conclusions

Before breakthrough, effluent concentrations of monovalent ions from the mixed bed are lower than the effluent concentrations of monovalent ions from any configuration of homogeneous beds studied. The results seem to indicate that, in the case of monovalent counterions, performance close to the mixed-bed performance is achieved if the ion-exchange bed exchanging the counterions in question is placed downstream from the bed that exchanges ions of opposite charge. For instance, in the case of sodium, initial leakages as low as those from mixed-bed are achieved if the cation-exchange bed is placed down stream of the anion-exchange bed. Similarly, in the case of chloride, initial leakage as low as that from mixed-bed are achieved if anion-exchange bed is placed down stream of cation-exchange bed. However, the same cannot be said of calcium or sulfate ions.

At lower concentrations, the differences between the leakages from different configurations observed for monovalent ions, are less pronounced as compared to the

differences at high concentrations. For instance, at higher feed concentrations, the sodium leakage from CAB is four orders of magnitude higher than the sodium leakage from MB. Similarly, at higher concentrations, chloride leakage from ACB is four orders of magnitude higher than the chloride leakage from MB. However, these differences are not as pronounced for the case of lower feeds concentrations. This could be because of the progressively reducing effect of the coions on the rate of ion exchange as the solution reaches the ideal state of infinite dilution where the coions will have no effect at all on the ion-exchange rate. The pH changes involved at low concentrations are also much smaller than those at higher concentrations and therefore, are expected to have a smaller effect on the equilibrium at low concentrations.

The order of the beds in the homogeneous-bed train affects the effluent pH also (besides the effluent concentrations). Before breakthrough, the pH of the effluent from the mixed bed is found to be closer to neutral than the pH of effluent from homogeneous-bed trains.

BIBLIOGRAPHY

- Beardsley S. S., Coker S. D. and Whipple S. S. (1995). Demineralization: The economics of reverse osmosis and ion exchange. Ultrapure Water, 12 (2), March 1995.
- Bhandari, V. M., Juvekar, V. A., Patwardhan, S. A., (1992 a). Sorption studies on ion exchange resins. 1. Sorption of strong acids on weak base resins. Ind. Eng. Chem. Res., 31 (4), 1060-1072.
- Bhandari, V. M., Juvekar, V. A., Patwardhan, S. A., (1992 b) Sorption studies on ion exchange resins. 2 Sorption of weak acids on weak base resins Ind. Eng. Chem. Res., 31 (4), 1073-1080.
- Bhandari, V. M., Juvekar, V. A., Patwardhan, S. A., (1993). Sorption of dibasic acids on weak base resins. Ind. Eng. Chem. Res., 32 (1), 200-206
- Blickenstaff, R. A., Wagner, J. D. and Dranoff, J. S. (1967 a). The kinetics of ion exchange accompanied by irreversible reaction. I. Film diffusion controlled neutralization of a strong acid exchanger by strong bases. The Journal Of Physical Chemistry, 71 (6), 1665-1669
- Blickenstaff, R. A., Wagner, J. D. and Dranoff, J. S. (1967 b). The kinetics of ion exchange accompanied by irreversible reaction. II. Intraparticle diffusion controlled neutralization of a strong acid exchanger by strong bases. The Journal of Physical Chemistry, 71 (6), 1670-1675
- Blumberg, R. (1984) Chemical Processing: acid-base salt systems. Ion Exchange Technology, Society Of Chemical Industry, London, 354 - 359.
- Bulusu, R. (1994). Development of a column model to predict multicomponent mixed bed ion exchange breakthrough. M.S. thesis, Oklahoma State University.
- Chowdiah, V. N., (1996). Liquid-film diffusion controlled ion-exchange modeling – Study of weak electrolyte mass transport and film mass-transfer kinetics. Ph.D. Dissertation, Oklahoma State University.
- Cutler, F. M. and Covey, J. N. (1995). Ion Exchange : Deoxygenation at ambient temperature. Ultrapure Water, 12 (4).

- Divekar, S. V., Foutch, G. L. and Haub, C. E. (1987). Mixed bed ion exchange at concentrations approaching the dissociation of water. Temperature effects. Ind. Eng. Chem. Res., 26 (9), 1906 - 1909.
- Dwivedi, P. N. and Upadhyay, S. N. (1977). Particle-Fluid Mass Transfer in Fixed and Fluidized Beds. Ind. Eng. Chem., Process Des. Dev., 16(2), 157-165.
- Fernandez, A., Rendueles, M., Rodrigues, A. and Diaz, M. (1994). Co-ion behavior at high concentration cationic ion exchange. Ind. Eng. Chem. Res., 33 (11), 2789-2794.
- Fernandez, A., Diaz, M. and Rodrigues, A. (1995). Kinetic mechanisms in ion exchange processes. The Chemical Engineering Journal, 57, 17-25
- Fisher, S. (1993). Track resin health to gage feedwater-demineralizer performance. Power, March 1993, 80-88.
- Franzreb, M., Holl, W. H. and Sontheimer, H. (1993). Liquid-phase Mass Transfer In Multi-component ion exchange. I. Systems Without Chemical Reactions In The Film. Reactive Polymers, 21, 117-133.
- Golden, L. (1986). Industrial use of ion exchange resins. The Chemical Engineer, October 1986, 31-34.
- Harfst, W. F. (1995). Back to basics : Controlling condensate corrosion without chemicals. Ultrapure Water, 12 (4), 1995.
- Haub, C. E. (1984). Model development for liquid resistance-controlled reactive ion exchange at low solution concentrations with applications to mixed bed ion exchange. M.S. Thesis, Oklahoma State University.
- Haub, C. E. and Foutch, G. L. (1986 a). Mixed-bed ion exchange at concentrations approaching the dissociation of water. 1. Model development. Ind. Eng. Chem. Fundam., 25, 373 - 381
- Haub, C. E. and Foutch, G. L. (1986 b). Mixed-bed ion exchange at concentrations approaching the dissociation of water. 2. Column model applications. Ind. Eng. Chem. Fundam., 25, 381 - 385.
- Helfferich, F. G. (1962) Ion Exchange. McGraw Hill Book Company, New York.
- Helfferich, F. G. (1984). Conceptual view of column behavior in multicomponent adsorption or ion-exchange systems. AIChE Symposium Series, 80 (233), 1-13.

- Helfferich, F. G. and Hwang, Y. L. (1985). Kinetics of acid uptake by weak-base anion exchangers. Mechanism of proton transfer. *AIChE Symposium Series*, 81 (242), 17-27.
- Kataoka, T., Yoshida, H. and Shibahara, Y. (1976). Liquid Phase Mass Transfer In Ion Exchange Accompanied By Chemical Reaction. *Journal Of Chemical Engineering Of Japan*, 9 (2), 130-135.
- Kraaijeveld, G. and Wesselingh, J. A. (1992). The kinetics of film-diffusion limited ion exchange. *Chemical Engineering Science*, 48 (3), 467-473.
- Liberti, L., Petruzelli, D., Helfferich, F. G. and Passino, R. (1987). Chloride/Sulfate ion exchange kinetics at high solution concentration. *Reactive Polymers*, 5, 37-47.
- Lou, J. (1993) Simulations of borate ion exchange and radial flow for reactor water clean up systems, M.S. Thesis, Oklahoma State University
- Okouchi, S., Yamanaka, K., Ishihara, Y., Yanaka, T. and Uedaira, H (1994). Relationship between water qualities and treatments in the ultra pure water production system. *Wat. Sci. Tech.*, 30 (10), 237-241.
- Petruzelli, D., Liberti, L., Passino, R., Helfferich, F. G. and Hwang, Y. L. (1987). Chloride/Sulfate exchange kinetics: Solution for combined film and particle diffusion control *Reactive Polymers*, 5, 219-226.
- Pondugula, S. K. (1994). Mixed bed ion exchange modeling for divalent ions in a ternary system. M.S. thesis, Oklahoma State University.
- Sadler, M. A. (1993) Developments in the production and control of ultrapure water. *Ion Exchange Processes : Advances and Applications*, A. Dyer, M. J. Hudson and P. A. Williams, Editors, The Royal Society of Chemistry, Cambridge, UK, 15-28.
- Yoon, T. K. (1990). The effect of cation to anion resin ratio on mixed-bed ion exchange performance at ultra-low concentrations, Ph.D. Dissertation, Oklahoma State University.
- Zecchini, E. J. (1990). Solutions to selected problems in multi-component mixed bed ion exchange modeling. Ph.D. Dissertation, Oklahoma State University.

APPENDIX A

INTERFACIAL CONCENTRATIONS AND ION-EXCHANGE EQUILIBRIA

The assumption of local equilibrium at the solid-liquid interface allows us to apply the law of mass action to resin-phase and interfacial concentrations. Thus, for an ion-exchange reaction,



the law of mass action is written as,

$$K_A^{B1} = \left(\frac{q_B}{C_B^*} \right)^{z_A} \left(\frac{C_A^*}{q_A} \right)^{z_B} \quad (\text{A-2})$$

The equilibrium constant for the ion-exchange reaction is called the selectivity coefficient.

Define the resin-phase and interfacial ionic equivalent fractions for ion A as,

$$y_A = \frac{q_A}{Q} \quad (\text{A-3})$$

$$X_A^* = \frac{C_A^*}{C_T^*}$$

Writing Equation A-2 in terms of equivalent fractions gives,

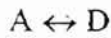
$$K_A^{B1} = \left(\frac{y_B}{X_B^*} \right)^{z_A} \left(\frac{X_A^*}{y_A} \right)^{z_B} Q^{(z_A - z_B)} C_T^{*(z_B - z_A)} \quad (\text{A-4})$$

The interfacial equivalent fraction of an ionic species B can now be written as,

$$X_B^* = y_B (K_A^B)^{z_B/z_A} \left(\frac{X_A^*}{y_A} \right)^{z_B/z_A} \left(\frac{Q}{C_T^*} \right)^{1-(z_B/z_A)} \quad (A-5)$$

where, initial resin loadings y_B and y_A , the resin capacity Q and selectivity coefficient are known (properties of the resin determined by experiment or known from manufacturer's specification).

We can also write relations similar to Equation A-5 for additional exchange reactions. Consider the following reactions,



where, A is the counterion in the resin phase and counterions B, C, D, E from the bulk phase are exchanging with A. Then, selectivity relationships for these reactions will give,

$$X_C^* = y_C (K_A^C)^{z_C/z_A} \left(\frac{X_A^*}{y_A} \right)^{z_C/z_A} \left(\frac{Q}{C_T^*} \right)^{1-(z_C/z_A)} \quad (A-6)$$

$$X_D^* = y_D (K_A^D)^{z_D/z_A} \left(\frac{X_A^*}{y_A} \right)^{z_D/z_A} \left(\frac{Q}{C_T^*} \right)^{1-(z_D/z_A)} \quad (A-7)$$

$$X_E^* = y_E (K_A^E)^{z_E/z_A} \left(\frac{X_A^*}{y_A} \right)^{z_E/z_A} \left(\frac{Q}{C_T^*} \right)^{1-(z_E/z_A)} \quad (A-8)$$

For any counterion i exchanging with A,

$$X_i^* = y_i (K_A^i)^{z_A/z_i} \left(\frac{X_A^*}{y_A} \right)^{z_A/z_i} \left(\frac{Q}{C_T^*} \right)^{1-(z_A/z_i)} \quad (\text{A-9})$$

$$\lambda_i = y_i (K_A^i)^{-1/z_A} (y_A)^{z_A/z_i} \left(\frac{Q}{C_T^*} \right)^{1-z_i/z_A} \quad (\text{A-10})$$

The material balance at the resin-liquid interface is,

$$\sum_{i=1}^n X_i^* - 1 = 0 \quad (\text{A-11})$$

Thus, there are $n-1$ equilibrium relations for n counterions involved in the exchange and one material balance equation. Substitute the $n-1$ equilibrium equations (Equations A-5 to A-8 in this case) into the material balance Equation A-9 to obtain a polynomial in terms of X_A^* .

$$X_A^* + \lambda_B (X_A^*)^{z_B/z_A} + \lambda_C (X_A^*)^{z_C/z_A} + \lambda_D (X_A^*)^{z_D/z_A} + \lambda_E (X_A^*)^{z_E/z_A} = 1 \quad (\text{A-12})$$

The coefficients of the terms of the polynomial are defined in Equation A-10. If the total interfacial concentration C_T^* is known, then the coefficients of the polynomial can be evaluated and the polynomial can be solved to obtain the interfacial equivalent fractions. Ion-exchange equilibrium is a function of total interfacial concentration which is unknown and must be found from the ionic flux rates. The flux rates in turn depend on the interfacial concentration and bulk concentration (as shown in Appendix B). Thus, it is necessary to start with a guess value for the total interfacial ionic concentration and find the correct value by iteration (as described in Table V).

APPENDIX B

MODEL EQUATIONS

We have assumed that liquid film diffusion is the rate controlling step for the ion exchange process. Therefore, the rate of change of concentration of an ionic species in the resin is same as the rate of diffusion of that species of ion through the liquid film.

Thus,

$$\frac{d\bar{C}_i}{dt} = -J_i a_s \quad (\text{B-1})$$

The equivalent fraction of ions in the resin is given by

$$y_i = \frac{z_i C_i}{Q} \quad (\text{B-2})$$

Replacing the resin phase concentration of ions in Equation B-1 by equivalent fraction of the ions in the resin (Equation B-2) yields

$$\frac{d y_i}{dt} = - \frac{z_i J_i a_s}{Q} \quad (\text{B-3})$$

The flux of counterions across the liquid film J_i is modeled by the Nernst-Planck equation as :

$$J_i = -D_i \left(\frac{\partial C_i}{\partial r} + \frac{C_i z_i F}{RT} \frac{\partial \phi}{\partial r} \right) \quad (\text{B-4})$$

Assumption of pseudo steady state lets us use ordinary differentials instead of partial differentials. Thus, the Nernst-Planck equation for the flux of counterions across the liquid film is now written as

$$J_i = -D_i \left(\frac{dC_i}{dr} + \frac{C_i z_i F}{RT} \frac{d\phi}{dr} \right) \quad (\text{B-5})$$

Similarly, for coion flux

$$J_j = -D_j \left(\frac{dC_j}{dr} + \frac{C_j z_j F}{RT} \frac{d\phi}{dr} \right) \quad (\text{B-6})$$

We can substitute the flux of counterions J_i in Equation B-3 by the Nernst-Planck Equation (B-5). However, we first eliminate the term for gradient in electrical potential ($d\phi/dr$) in Equation B-5.

Elimination of Term for Gradient in Electrical Potential

Assumption of electroneutrality in the liquid film gives equal concentration of counterions and coions in the film:

$$\sum_{i=1}^n z_i C_i = \sum_{j=1}^m z_j C_j \quad (\text{B-7})$$

Assumption of no coion flux in the liquid film yields

$$z_j J_j = 0 \quad (\text{B-8})$$

Also, assumption of no net current flow in the film can be written mathematically as :

$$\sum_{i=1}^n z_i J_i = \sum_{j=1}^m z_j J_j \quad (\text{B-9})$$

From Equation B-8 and Equation B-9,

$$\sum_{i=1}^n z_i J_i = \sum_{j=1}^m z_j J_j = 0 \quad (\text{B-10})$$

Thus, the sum of equivalent fluxes of counterions and the sum of equivalent fluxes of coions is zero. From Equation B-6 and Equation B-10, the gradient of electrical potential is

$$\frac{d\phi}{dr} = \frac{-RT}{F} \left(\frac{\sum_{j=1}^m z_j \frac{dC_j}{dr}}{\sum_{j=1}^m z_j^2 C_j} \right) \quad (\text{B-11})$$

The total equivalent concentration of counterions is equal to that of coions because we assume electroneutrality in the liquid film. The total equivalent concentration is given by

$$C_T = \omega \sum_{i=1}^n z_i C_i = \omega \sum_{j=1}^m z_j C_j \quad (\text{B-12})$$

The mean value for coion valence is defined as .

$$z_y = \left(\frac{\sum_{j=1}^m z_j^2 C_j}{\sum_{j=1}^m z_j C_j} \right) \quad (\text{B-13})$$

From Equation B-12 and Equation B-13

$$\sum_{j=1}^m z_j^2 C_j = z_y C_T \quad (\text{B-14})$$

Differentiating Equation B-12 with respect to distance in the film,

$$\frac{dC_T}{dr} = \sum_{j=1}^m z_j \frac{dC_j}{dr} \quad (\text{B-15})$$

Substitute Equations B-15 and B-14 into Equation B-11 to get

$$\frac{d\phi}{dr} = \frac{-RT}{z_y F C_T} \frac{dC_T}{dr} \quad (\text{B-16})$$

Now, the Nernst-Planck equation for counterion flux (Equation B-5) can be written as

$$J_i = -D_i \left(\frac{dC_i}{dr} - \frac{C_i z_i}{C_T z_y} \frac{dC_T}{dr} \right) \quad (\text{B-17})$$

Thus, the term for the gradient in electrical potential has been replaced by a function of total equivalent concentration. In order to evaluate the ionic flux rates J_i , it is now necessary to find a relation between the total equivalent concentration C_T and the individual ionic concentration C_i .

Finding Relation between Total Equivalent Concentration and Individual Ionic Concentrations

Define the relative valences for the counterions as

$$N_i = -\frac{z_i}{z_y} \quad (\text{B-18})$$

Equation B-10 can be combined with Equation B-17 to get

$$\sum_{i=1}^n z_i J_i = \sum_{i=1}^n z_i D_i \frac{dC_i}{dr} + \frac{dC_T}{dr} \frac{1}{C_T} \sum_{i=1}^n z_i D_i N_i C_i = 0 \quad (\text{B-19})$$

For the case of a monovalent system of ions involved in ion exchange, this equation can be integrated to obtain a relation between C_i and C_T . However, integration is not possible in the case of arbitrary valences. So we use the method of Franzreb et al. (1993). This method yields a solution which is exact for the case of monovalent system of ions. The solution given by this method (Franzreb et al., 1993) for the case of counterions with arbitrary valences is only approximate.

Case I (Counterions having equal valences)

Differentiate Equation B-17 with respect to distance in the film, and substitute Equation B-18. The flux of an ionic species does not change with distance in the film because of mass balance and from our assumption that curvature of the film is negligible. Therefore, derivative of J_i with respect to distance in the film is zero

$$\frac{d^2C_i}{dr^2} + \frac{N_i}{C_T} \frac{dC_i}{dr} \frac{dC_T}{dr} + N_i \frac{C_i}{C_T} \left(\frac{d^2C_T}{dr^2} - \frac{1}{C_T} \left(\frac{dC_T}{dr} \right)^2 \right) = 0 \quad (\text{B-20})$$

Summation of Equation B-20 for all counterions leads to the following equation

$$\sum_{i=1}^n \frac{d^2C_i}{dr^2} + \frac{1}{C_T} \frac{dC_T}{dr} \sum_{i=1}^n N_i \frac{dC_i}{dr} + \frac{1}{C_T} \frac{d^2C_T}{dr^2} \sum_{i=1}^n N_i C_i - \frac{1}{C_T^2} \left(\frac{dC_T}{dr} \right)^2 \sum_{i=1}^n N_i C_i = 0 \quad (\text{B-21})$$

On applying Equation B-12 and its derivatives, Equation B-20 reduces to

$$\frac{d^2C_T}{dr^2} = 0 \quad (\text{B-22})$$

From Equation B-22, we know that, the total equivalent concentration of ions in the liquid film varies linearly with distance in the film for the case of counterions with equal valences. Therefore,

$$\frac{dC_T}{dr} = m_g \quad (\text{B-23})$$

where m_g is a constant. We can now express the derivatives of C_i with respect to distance in the film in terms of derivatives with respect to C_T and we can write Equation B-20 as

$$\frac{d^2 C_i}{dC_T^2} + \frac{N_i}{C_T} \frac{dC_i}{dC_T} - \frac{N_i C_i}{C_T^2} = 0 \quad (\text{B-24})$$

This expression is of the same form as Euler's differential equation and its solution is

$$z_i C_i = A_i C_T + B_i C_T^{-P} \quad (\text{B-25})$$

where P is N_i for the case of equal valences of counterions. The values of the parameters A_i and B_i in Equation B-25 are found by applying the boundary conditions for the liquid film,

$$\begin{aligned} \text{at } r = 0, \quad C_T &= C_T^* \\ \text{at } r = \delta, \quad C_T &= C_T^0 \end{aligned} \quad (\text{B-26})$$

The values of A_i and B_i are,

$$\begin{aligned} A_i &= \frac{1}{C_T^0} \left(z_i C_i^0 - B_i (C_T^0)^{-P} \right) \\ B_i &= \omega \left(\frac{X_i^* - X_i^0}{(C_T^*)^{-P-1} - (C_T^0)^{-P-1}} \right) \end{aligned} \quad (\text{B-27})$$

From Equations B-25 and B-27 we now know the individual ionic concentration C_i in terms of total equivalent concentration C_T . Substitute C_i and its derivative in the

modified Nernst-Planck flux expression (Equation B-17) with Equation B-25 and its derivative,

$$J_i = -\frac{D_i}{z_i} \frac{dC_T}{dr} \left[(A_i - PB_i C_T^{-P-1}) + N_i (A_i + B_i C_T^{-P-1}) \right] \quad (\text{B-28})$$

Substitute P by N_i in Equation B-28 for the case of counterions with equal valences. For case I, Franzreb has derived the expression for total equivalent concentration at the resin surface to be,

$$C_T^* = \left[\frac{\sum_{i=1}^n D_i X_i^0}{\sum_{i=1}^n D_i X_i^*} \right]^{\frac{1}{P+1}} C_T^0 \quad (\text{B-29})$$

Case II (Counterions having unequal valences)

In this case, the total equivalent concentration in the liquid film does not vary linearly with distance in the film. We may still apply Equation B-25 developed for the case of equal counterion valences, but, with a different value for P as given by Franzreb

Substitute Equation B-28 into Equation B-10,

$$\left(\sum_{i=1}^n D_i A_i + \sum_{i=1}^n N_i D_i A_i \right) + \left(\sum_{i=1}^n N_i D_i B_i - P \sum_{i=1}^n D_i B_i \right) C_T^{-P-1} = 0 \quad (\text{B-30})$$

For Equation B-30 to be true, both the terms in the parentheses must be zero. Thus,

$$\sum_{i=1}^n (1 + N_i) D_i A_i = 0 \quad (\text{B-31})$$

$$\left(\sum_{i=1}^n N_i D_i B_i - P \sum_{i=1}^n D_i B_i \right) = 0 \quad (\text{B-32})$$

For case I (equal counterion valences), an equation similar to B-31 can be derived:

$$\sum_{i=1}^n D_i A_i = 0 \quad (\text{B-33})$$

Comparison of Equations B-31 and B-33 shows that $(1+N_i) D_i$ in case II replaces D_i of case I. Therefore, we can replace D_i with $(1+N_i) D_i$ in the expression for total equivalent concentration at the resin surface (Equation B-29) as follows :

$$C_T^* = \left[\frac{\sum_{i=1}^n (1+N_i) D_i x_i^0}{\sum_{i=1}^n (1+N_i) D_i x_i^*} \right]^{\frac{1}{P+1}} C_T^0 \quad (\text{B-34})$$

Also, P for Case II is obtained by substituting for B_i (Equation B-27) in Equation B-32,

$$P = \frac{\sum_{i=1}^n N_i D_i (x_i^* - x_i^0)}{\sum_{i=1}^n D_i (x_i^* - x_i^0)} \quad (\text{B-35})$$

Similar to case I, integration of the modified Nernst-Planck Equation (B-17) with boundary conditions (Equation B-26) and substitution of P (Equation B-35) gives,

$$J_i = \frac{D_i}{\delta} \left[\left(1 - \frac{N_i}{P} \right) (C_i^* - C_i^0) + N_i \frac{A_i}{Z_i} \left(1 + \frac{1}{P} \right) (C_T^* - C_T^0) \right] \quad (\text{B-36})$$

We now know the individual ionic flux rates in the liquid film (J_i) in terms of interfacial and bulk liquid concentrations (Equation B-36). The liquid film thickness in Equation B-36 is still an unknown and is eliminated as follows :

$$\delta = D_e / k \quad (\text{B-37})$$

Therefore,

$$\frac{J_i}{k} = \frac{D_i}{D_e} \left[\left(1 - \frac{N_i}{P} \right) (C_i^* - C_i^0) + N_i \frac{A_i}{Z_i} \left(1 + \frac{1}{P} \right) (C_T^* - C_T^0) \right] \quad (\text{B-38})$$

where the effective diffusivity D_e is defined as,

$$D_e = \frac{\sum_{i=1}^n |J_i \delta|}{\sum_{i=1}^n |C_i^* - C_i^0|} \quad (\text{B-39})$$

and the mass transfer coefficient k is given by the correlation of Dwivedi and Upadhyay (1977),

$$k = \left(\frac{D_e}{d_p} \right) Sc^{1/3} R \left[\frac{0.765}{(eR)^{0.82}} + \frac{0.365}{(eR)^{0.386}} \right] \quad (\text{B-40})$$

The J_i for each species is found using Equations B-38 and B-40. The rate of loading of the resin beads can then be evaluated from Equation B-3.

APPENDIX C

MATERIAL BALANCE EQUATIONS

A material balance for the ion exchange column must be setup in order to predict the effluent concentration with time. The differential column material balance can be viewed as a material balance applied to a very small slice of the resin column. The net increase or decrease in the amount of an ionic species present in the resin in the slice equals the net influx or efflux of the ionic species from the bulk solution. The material balance equation for exchange of ion i between the resin bed and the solution phase is written as,

$$\frac{u_s}{\varepsilon} \frac{\partial C_i}{\partial Z} + \frac{\partial C_i}{\partial t} + \frac{(1-\varepsilon)}{\varepsilon} \frac{\partial q_i}{\partial t} = 0 \quad (\text{C-1})$$

Define dimensionless variables for any ion i as,

$$\tau = \frac{k_i C_T^i}{d_p Q} \left(t - \frac{\varepsilon Z}{u_s} \right)$$

and, (C-2)

$$\varepsilon = \frac{k_i (1-\varepsilon) Z}{u_s d_p}$$

In order to write the column material balance in terms of dimensionless variables, the differentials of ordinary variables must be expressed in terms of differentials of dimensionless variables. Differentiating the expressions in Equation C-2,

$$\frac{\partial \tau}{\partial t} = \frac{k_i C_T^f}{d_p Q}$$

$$\frac{\partial \tau}{\partial Z} = -\frac{k_i C_T^f \varepsilon}{d_p Q u_s}$$

$$\frac{\partial \xi}{\partial t} = 0$$

$$\frac{\partial \xi}{\partial Z} = \frac{k_i (1 - \varepsilon)}{d_p u_s} \quad (C-3)$$

Evaluate the differentials of ordinary variables in terms of differentials of dimensionless variables using the chain rule and equations C-3,

$$\frac{\partial C_1}{\partial Z} = \frac{\partial C_1}{\partial \xi} \frac{\partial \xi}{\partial Z} + \frac{\partial C_1}{\partial \tau} \frac{\partial \tau}{\partial Z}$$

$$\frac{\partial C_1}{\partial Z} = \frac{\partial C_1}{\partial \xi} \left(\frac{k_i (1 - \varepsilon)}{d_p u_s} \right) + \frac{\partial C_1}{\partial \tau} \left(-\frac{k_i C_T^f \varepsilon}{d_p Q u_s} \right)$$

$$\frac{\partial C_1}{\partial t} = \frac{\partial C_1}{\partial \xi} \frac{\partial \xi}{\partial t} + \frac{\partial C_1}{\partial \tau} \frac{\partial \tau}{\partial t}$$

$$\frac{\partial C_1}{\partial t} = \frac{\partial C_1}{\partial \tau} \left(\frac{k_i C_T^f}{d_p Q} \right) \quad (C-4)$$

$$\frac{\partial q_1}{\partial t} = \frac{\partial q_1}{\partial \xi} \frac{\partial \xi}{\partial t} + \frac{\partial q_1}{\partial \tau} \frac{\partial \tau}{\partial t}$$

$$\frac{\partial q_1}{\partial t} = \frac{\partial q_1}{\partial \tau} \left(\frac{k_i C_T^f}{d_p Q} \right)$$

Substitute the differentials of ordinary variables Z and t in terms of differentials of τ and ξ from equations C-4 to get,

$$\frac{\partial C_i}{\partial \xi} + \frac{C_T^f}{Q} \frac{\partial q_i}{\partial \tau} = 0 \quad (\text{C-5})$$

Define equivalent fractions in resin and bulk phase as,

$$x_i = \frac{C_i}{C_T^f} \quad (\text{C-6})$$

$$y_i = \frac{q_i}{Q}$$

Substitute equivalent fractions for concentrations into Equation C-5.

$$\frac{\partial x_i}{\partial \xi} + \frac{\partial y_i}{\partial \tau} = 0 \quad (\text{C-7})$$

The material balance equation C-7 is written for any ion i . Similar equations may be written for all ions passing through the column. However, solution of all the material balance equations must proceed with the same step sizes in time and distance because the flux expressions for all the ions are linked to the concentrations of other species and determination of fluxes requires bulk concentration and resin loadings of all species of ions at that time and depth in the column. Therefore, it is necessary to write the material balance equations for all the ions in terms of the same dimensionless variables τ and ξ . A reference ion is chosen for this purpose and the material balance equations are written in terms of the dimensionless variables defined for the reference ion. In this study, chloride was chosen as the reference ion for the anion exchange bed and sodium was chosen for cation exchange beds.

Dimensionless variables for the reference ion r are,

$$\tau_r = \frac{k_r C_T^f}{d_p Q} \left(t - \frac{\varepsilon Z}{u_s} \right)$$

and,

$$\varepsilon_r = \frac{k_r (1 - \varepsilon) Z}{u_s d_p}$$
(C-8)

Writing the differentials for any ion i in terms of the dimensionless variables for the reference ion r,

$$\frac{\partial X_i}{\partial \xi_i} = \frac{\partial X_i}{\partial \xi_r} \left(\frac{\partial \xi_r}{\partial \xi_i} \right) = \frac{\partial X_i}{\partial \xi_r} \frac{k_r}{k_i}$$

$$\frac{\partial y_i}{\partial \tau_i} = \frac{\partial y_i}{\partial \tau_r} \left(\frac{\partial \tau_r}{\partial \tau_i} \right) = \frac{\partial y_i}{\partial \tau_r} \frac{k_r}{k_i}$$
(C-9)

Thus, column material balance equation for the ion i is now,

$$\frac{\partial X_i}{\partial \xi_r} \frac{k_r}{k_i} + \frac{\partial y_i}{\partial \tau_r} \frac{k_r}{k_i} = 0$$
(C-10)

Divide Equation C-10 by (k_r/k_i) ,

$$\frac{\partial X_i}{\partial \xi_r} + \frac{\partial y_i}{\partial \tau_r} = 0$$
(C-11)

Modification of Flux Expressions to Incorporate the Dimensionless Variables

The rate of resin loading for ion i is related to its flux across the liquid film as,

$$\frac{d y_i}{d t} = - \frac{Z_i J_i a_s}{Q}$$
(C-12)

Substituting dimensionless variable for ion i,

$$\frac{dy_i}{d\tau_i} = \left(-\frac{z_i J_i a_s}{Q} \right) \frac{dt}{d\tau_i} \quad (C-13)$$

$$\frac{dy_i}{d\tau_i} = \left(-\frac{z_i J_i a_s}{Q} \right) \frac{d_p Q}{k_i C_T^i}$$

Now, substitute dimensionless variable for reference ion r,

$$\frac{dy_i}{d\tau_i} = \left(-\frac{z_i J_i a_s}{Q} \right) \frac{d\tau_i}{d\tau_r}$$

$$\frac{dy_i}{d\tau_i} = \left(-\frac{z_i J_i a_s}{Q} \right) \frac{d_p Q}{k_i C_T^i} \frac{k_r}{k_r} \quad (C-14)$$

$$\frac{dy_i}{d\tau_{ii}} = \left(-\frac{z_i J_i a_s d_p}{C_T^i k_r} \right)$$

Note that $a_s d_p = 6$, if we assume spherical resin beads. Thus,

$$\frac{dy_i}{d\tau_{ii}} = \left(-\frac{6 z_i J_i}{C_T^i k_r} \right) \quad (C-15)$$

The flux of ions across the liquid film is evaluated and substituted into Equation C-15 to find the rate of resin loading. The dimensionless material balance combined with Equation C-15 will enable us to predict the effluent concentration histories and also the profile of resin loading along the length of the column at any time.

APPENDIX D

NUMERICAL METHODS

The column material balance equation must be applied to each ionic species in order to obtain the effluent concentration history or the resin loading profile across the length of the column. This requires integration of a system of partial differential equations of the form,

$$\frac{\partial X_i}{\partial \xi_r} + \frac{\partial y_i}{\partial \tau_r} = 0 \quad (\text{D-1})$$

The differential equation involves two independent variables, τ and ξ . The method of characteristics is used to integrate the system of material balance equations. This method involves integration with respect to one variable, keeping the other variable constant. Thus, the partial differential equation is considered to be an ordinary differential equation in terms of one variable and integrated while the other variable is being kept constant. The integration of the material balance can be divided into two tasks:

1. integration to obtain liquid phase concentrations along the length of the column at constant time
2. integration to obtain resin loading at the next step in time for the same depth in the column

Zechhini (1990) has conducted a thorough survey of numerical methods for carrying out integration of the differential equations and Pondugula (1992) has justified the choice of numerical methods used in the current model. The explicit Euler method is used to predict resin loading in the HBIE model, and Gear's backward difference method of fourth order is used for the liquid phase concentrations.

APPENDIX E

SIMULATION OF HOMOGENEOUS BEDS IN SERIES

The code for simulating HBIE can be adapted for simulation of ion-exchange beds in series. Ion-exchange trains consisting of one cationic-resin bed and one anionic-resin bed in series are simulated and the effect of the order of the beds on the effluent water quality is studied. The performance of a mixed-bed unit (predicted by MBIE model) is also compared with the performance of homogeneous beds in series. The procedure used for these simulations is outlined here.

For the simulation of beds in series, separate programs are run for each bed. The history of effluent ionic concentrations predicted by the first program is written to an interface file which is read by the second program. In this regard, one has to keep in mind the following points

1. The second program must be capable of handling a variable feed condition because the output from one bed is being fed to the second bed.
2. The step sizes used to integrate the material balances for the two beds must be the same in terms of time. However, the step size in terms of distance can vary between the two codes for beds in series.

Thus, the time interval (Δt) between two consecutive effluent concentrations generated by the first program must be the same as the step size in time used by the second program.¹ The integration procedure is very sensitive to the step size. Therefore, both programs must be run with a very small step size in time.

¹ Note that the time mentioned here is not the program run time, but real time for the bed runs.

APPENDIX F

COMPUTER CODE

```
*****
*
*
*   THIS PROGRAM IS USED FOR PREDICTING THE EFFLUENT
*   CONCENTRATIONS FOR A MULTICOMPONENT SYSTEM OF
*   IONS EXCHANGING IN A HOMOGENEOUS BED OF ANION-
*   EXCHANGE RESIN
*
*   OUTPUT FROM THIS CODE GOES TO INTERFACE.DAT WHICH IS
*   USED AS INPUT FOR CATIONIC RESIN BED. THE 2 BEDS ARE IN
*   SERIES.
*
*   DEVELOPED BY :
*   ASHWIN P G &
*   DR. GARY L. FOUTCH
*
*****
*
*   C - PREFIX FOR CATONS; A - PREFIX FOR ANIONS
*
*****
```

IMPLICIT INTEGER (I-N), REAL*8 (A-H,O-Z)

```
COMMON CBC(20), CBA(20)
COMMON TKC(20), TKA(20), DC(20), DA(20), ZC(20), ZA(20)
COMMON RC(20), RA(20), CF, QC, QA, DRC, DRA, SUMYC, SUMYA
COMMON DISS, CBH, CBOH, DH, DOH, Z1, Z2,NC,NA
REAL*8 RTC, RTA(20,4,6500), MC(20), MA(20),
1   CFC(20),CFA(20),YCO(20), YAO(20), COEC(20), COEA(20),
1   PPBC(20), PPBA(20),KREF, YACUR(20),
1   XACUR(20),YA(20,4,6500),XC(20),
```

```

1  XA(20,4,6500)
*
*  -----
*  Correlations- Dwivedi and Upadhyay
*  -----
F2(DR,R,S) = (DR/PDA) * (S**(1.0/3.0)) * R *
1  ((0.765/((VD*R)**0.82)) + (0.365/((VD*R)**0.386)))
*
*  -----
*  READING THE DATA
*  -----
OPEN(UNIT=9,FILE='animult.dat',STATUS = 'UNKNOWN')
OPEN(UNIT=8,FILE='interface.dat',STATUS='UNKNOWN')
READ(9,*)NC,NA,Z1,Z2,DH,DOH
READ(9,*)KPBK, KPPR, TIME
READ(9,*)PDA, VD
READ(9,*)FR, DIA, CHT
READ(9,*)TAU, XI, TMP
READ(9,*)DEN, QA

DO 2 II = 1,NC
  READ(9,*)YCO(II),CFC(II),ZC(II),MC(II),TKC(II)
  WRITE(*,*)YCO(II),CFC(II),ZC(II),MC(II),TKC(II)
2 CONTINUE

DO 3 JJ = 1,NA
  READ(9,*)YAO(JJ),CFA(JJ),ZA(JJ),MA(JJ),TKA(JJ)
  WRITE(*,*)YAO(JJ),CFA(JJ),ZA(JJ),MA(JJ),TKA(JJ)
3 CONTINUE

CP = 1.43123+TMP*(0.000127065*TMP-0.0241537)
ALOGKW = 4470.99/(TMP+273.15)-6.0875+0.01706*(TMP+273.15)
DISS = 10.**(-ALOGKW)

CALL EQB(CFC,CFA)
PH = 14.0 + LOG10(CBOH)
WRITE (*,*) 'PH of inlet soln =', PH

CF = 0.0
DO 8 JJ = 1,NA
  CF = CF + CFA(JJ)
8 CONTINUE
CF = CF+CBOH
WRITE (*,*) 'CF =',CF
RTF = (8.931D-10)*(TMP+273.16)

```

```

C
C SELF DIFFUSIVITIES OF IONS
C
C DC(1) = SODIUM, DC(2) = CALCIUM
C DA(1) = CHLORIDE, DA(2) = SULFATE
C
dc(1) =(RTF)*(23.00498+1.06416*TMP+0.0033196*TMP**2)
dc(2) =(RTF)*(23.27+1.575*TMP)/2.0
da(1) =(RTF)*(39.6493+1.39176*TMP+0.0033196*TMP**2)
da(2) =(RTF)*(35.76+2.079*TMP)/2.0

```

```

C
C kref is set to Cl ion.
C

```

```

kref = 0.01937466

```

```

AREA = 3.1415927*(DIA**2)/4.
VS = FR/AREA
RPA = PDA*100.*VS*DEN/((VD)*CP)
SCA = (CP/100.)/DEN/DA(1)

```

```

*
* -----
* CALCULATE TOTAL NUMBER OF STEPS IN DISTANCE (NT) DOWN
* COLUMN:SLICES
*

```

```

CHTD = KREF*(1.-VD)*CHT/(VS*PDA) !distance dimensionless
NT = CHTD/XI
WRITE (*,*)chtd,xi,nt

```

```

*
* SET INITIAL RESIN LOADING THROUGHOUT THE ENTIRE COLUMN
*

```

```

MT = NT + 1
DO 4 M=1,MT

```

```

    DO 6 JJ = 1,NA
      YA(JJ,1,M) = YAO(JJ)
6 CONTINUE

```

```

4 CONTINUE

```

```

*
* -----
* CALCULATE DIMENSIONLESS PROGRAM TIME LIMIT
* BASED ON INLET CONDITIONS (AT Z=0)
*

```

```

TMAX = 6.0*QA*3.142*(DIA/2.)**2.*CHT/(FR*CF*60.)
TAUMAX = KREF*CF*(TMAX*60.)/(PDA*QA)
DMAX=TMAX/1440.

```

```

WRITE(6,*)
WRITE(6,*)
WRITE(6,222)
WRITE(6,223)DMAX
WRITE(6,224)
222 FORMAT(' PROGRAM RUN TIME IS BASED ON TOTAL RESIN CAPACITY')
223 FORMAT(' AND FLOW CONDITIONS. THE PROGRAM WILL RUN
FOR',F12.1)
224 FORMAT(' DAYS OF COLUMN OPERATION FOR THE CURRENT
CONDITIONS.')
```

```

*
* _____
* INITIALIZE VALUES PRIOR TO ITERATIVE LOOPS
* _____
```

```

      J = 1
      JK = 1
      TAUTOT = 0.
      JFLAG = 0
      KK = 1
      KPRINT = 100
      CONS = -6./KREF/CF
      Dtime = TAU*PDA*QA/(KREF*CF*60.)/1440.
      write(8,*) Dtime  !time in days between 2 consecutive output values
```

```

*
* _____
* TIME STEP LOOP WITHIN WHICH ALL COLUMN CALCULATIONS ARE
* IMPLEMENTED TIME IS INCREMENTED AND OUTLET CONCENTRATION
* CHECKED
* _____
```

```

1  CONTINUE
   IF (TAUTOT.GT.TAUMAX) GOTO 138
   IF (J.EQ.4) THEN
     JD = 1
   ELSE
     JD = J + 1
   ENDIF
```

```

*
* _____
* SET INLET LIQUID PHASE FRACTIONAL CONCENTRATIONS FOR EACH
* SPECIES IN THE MATRIX
* _____
```

```

      DO 7 II = 1,NC
        XC(II) = CFC(II)/CF
7  CONTINUE
```

```
      DO 10 JJ = 1,NA
      XA(JJ,J,1) = CFA(JJ)/CF
10  CONTINUE
```

```
*
* _____
* LOOP TO INCREMENT DISTANCE (BED LENGTH) AT A FIXED TIME
* _____
```

```
      DO 400 K=1,(NT+4)

      If (K.EQ 1) then
          DO 11 II = 1,NC
          CBC(II)=XC(II)*CF
11      CONTINUE
      Endif

          DO 12 JJ = 1,NA
          CBA(JJ)=XA(JJ,J,K)*CF
12      CONTINUE
```

```
*
* _____
* CALL ROUTINES TO CALCULATE RN, RB, CNI, CBI(INTERFACIAL
* CONCENTRATIONS
* & COEFFICIENTS)
* _____
```

```
      DO 15 II = 1,NC
      RC(II) = 0.0
15  CONTINUE

      SUMYA = 0.0
      DO 14 JJ = 1,NA
      SUMYA = SUMYA+YA(JJ,J,K)
14  CONTINUE
```

```
      DO 29 JJ = 1,NA
      YACUR(JJ) = YA(JJ,J,K)
29  CONTINUE
```

```
      DO 30 JJ = 1,NA
      XACUR(JJ) = XA(JJ,J,K)
30  CONTINUE
```

```
      IF(SUMYA.LT.0.999)THEN
```

```
      CALL ANION(YACUR,XACUR,k)
```



```

ELSE

DO 16 JJ = 1,NA
RA(JJ) = 0.0
16 CONTINUE

ENDIF

SCA = (CP/100.)/DEN/DRA
AKA = F2(DRA,RPA,SCA)

DO 17 II = 1,NC
RTC = 0.0
17 CONTINUE

DO 18 JJ = 1,NA
RTA(JJ,J,K) = RA(JJ)*AKA*CONS
18 CONTINUE

DO 20 JJ = 1,NA
YA(JJ,JD,K) = YA(JJ,J,K)+TAU*RTA(JJ,J,K)
20 CONTINUE

```

```

*
* _____
* IMPLEMENT IMPLICIT PORTION OF THE GEARS BACKWARD DIFFERENCE
METHOD
* FROM THE PREVIOUS FUNCTION VALUES. FOR THE FIRST THREE STEPS
* USE FOURTH-ORDER RUNGE KUTTA METHOD
*
* _____

```

```

IF(K.LE.3)THEN

DO 22 JJ = 1,NA
XA(JJ,J,K+1) = XA(JJ,J,K)-(XI*RTA(JJ,J,K))
22 CONTINUE

ELSE

DO 24 JJ = 1,NA
COEA(JJ) = 3 *XA(JJ,J,K-3)/25. -16.*XA(JJ,J,K-2)/25. +
1 36.*XA(JJ,J,K-1)/25. -48.*XA(JJ,J,K)/25.
24 CONTINUE

```

```
DO 26 JJ = 1,NA
XA(JJ,J,K+1) = -XI*12.*RTA(JJ,J,K)/25.-COEA(JJ)
26 CONTINUE
```

```
ENDIF
```

```
*
```

```
* DETERMINE CONCENTRATIONS FOR THE DISTANCE STEP AND
RECALCULATE
```

```
* BULK PHASE EQUILIBRIA
```

```
*
```

```
DO 32 JJ = 1,NA
CBA(JJ)=XA(JJ,J,K+1)*CF
32 CONTINUE
```

```
CALL EQB(CBC,CBA)
```

```
400 CONTINUE
```

```
*
```

```
* PRINT BREAKTHROUGH CURVES
```

```
*
```

```
IF (KPBK.NE.1) GO TO 450
DO 45 II = 1,NC
PPBC(II) = CBC(II)*MC(II)/1.E-6
45 CONTINUE
```

```
DO 46 JJ = 1,NA
PPBA(JJ) = CBA(JJ)*MA(JJ)/1.E-6
46 CONTINUE
```

```
TAUTIM = TAUTOT*PDA*QA/(KREF*CF*60.)
PH = 14. + LOG10(CBOH)
```

```
write(8,48)CBC(1),CBC(2),CBH,CBA(1),CBA(2),CBOH,PH
48 FORMAT(1x,E12.7,2x,E12.7,2x,E12.7,2x,E12.7,2x,E12.7,2x,E12.7
1 ,2x,F5.2)
```

```
IF (KPRINT.NE.100) GOTO 450
WRITE(*,47)TAUTIM,PPBC(1),PPBC(2),PPBA(1),PPBA(2),PH
```

47 FORMAT(1x,F11.6,2X,E12.7,2X,E12.7,2X,E12.7,4X,E12.7,4X,F5.2)

*

* STORE EVERY TENTH ITERATION TO THE PRINT FILE

*

KPRINT = 0

450 CONTINUE

KPRINT = KPRINT+1

JK = J

IF (J.EQ.4) THEN

J = 1

ELSE

J = J+1

ENDIF

*

* END OF LOOP RETURN TO BEGINNING AND STEP IN TIME

*

IF (JFLAG.EQ.1) STOP

TAUTOT = TAUTOT + TAU

GOTO 1

138 STOP

END

SUBROUTINE EQB(CC,CA)

IMPLICIT INTEGER (I-N), REAL*8 (A-H,O-Z)

COMMON CBC(20), CBA(20)

COMMON TKC(20), TKA(20), DC(20), DA(20), ZC(20), ZA(20)

COMMON RC(20), RA(20), CF, QC, QA, DRC, DRA, SUMYC, SUMYA

COMMON DISS, CBH, CBOH, DH, DOH, Z1, Z2,NC,NA

REAL*8 CC(50),CA(50)

SUMC = 0.0

DO 1 II = 1,NC

SUMC = SUMC + CC(II)

1 CONTINUE

SUMA = 0.0

```
DO 2 JJ = 1,NA
SUMA = SUMA+CA(JJ)
2 CONTINUE
```

```
V1 = SUMC-SUMA
V2 = V1**2.+4.*DISS
```

```
CBOH = (V1+(V2**0.5))/2.
CBH = DISS/CBOH
```

```
RETURN
END
```

```
SUBROUTINE ANION(YY,XX,k)
```

```
IMPLICIT INTEGER (I-N), REAL*8 (A-H,O-Z)
```

```
COMMON CBC(20), CBA(20)
COMMON TKC(20), TKA(20), DC(20), DA(20), ZC(20), ZA(20)
COMMON RC(20), RA(20), CF, QC, QA, DRC, DRA, SUMYC, SUMYA
COMMON DISS, CBH, CBOH, DH, DOH, Z1, Z2,NC,NA
```

```
REAL*8 YY(50),XX(50),XXN(50),CCO(50),N(50),LAM(50),XXI(50),
1 BB(50),AA(50),CBN(50),CI(50),R1(50),NOH
```

```
W = -1.0
YOH = 1 -SUMYA
CTO = 0.0
DO 1 II = 1,NA
CTO = CTO+CBA(II)
1 CONTINUE
CTO = CTO+CBOH
```

```
DO 2 II = 1,NA
XXN(II) = XX(II)*CF/CTO
2 CONTINUE
```

```
SUMXB = 0.0
DO 3 II = 1,NA
SUMXB = SUMXB+XXN(II)
```

```

3  CONTINUE
   XBOH = 1. - SUMXB

   DO 4 JJ = 1,NC
   CCO(JJ) = CBC(JJ)/ABS(ZC(JJ))
4  CONTINUE
   CH = CBH/ABS(Z1)

   SUMZN = 0.0
   DO 5 JJ = 1,NC
   SUMZN = SUMZN+(ZC(JJ)**2.)*CCO(JJ)
5  CONTINUE
   SUMZN = SUMZN + (Z1**2.)*CH

   SUMZD = 0.0
   DO 6 JJ = 1,NC
   SUMZD = SUMZD+(ZC(JJ)*CCO(JJ))
6  CONTINUE
   SUMZD = SUMZD + (Z1*CH)

   ZY = SUMZN/SUMZD

   DO 7 II = 1,NA
   N(II) = -ZA(II)/ZY
7  CONTINUE
   NOH = -Z2/ZY

   CTI = CTO
8  CONTINUE

   DO 9 II = 1,NA
   LAM(II) = YY(II)*TKA(II)**(-1./ABS(Z2))*YOH**(-ZA(II)/Z2)
1  *(QA/CTI)**(1.-ZA(II)/Z2)
9  CONTINUE

C  NEWTON-RAPHSON SOLVER

   EPS = 1 E-07
   X = XBOH
   SUMFN = 0.0
   DO 10 II = 1,NA
   SUMFN = SUMFN + (LAM(II)*X**(ZA(II)/Z2))
10 CONTINUE
   SUMFN = SUMFN+X-1.0

```

```

SUMFD = 1.0
DO 11 II = 1,NA
SUMFD = SUMFD-((ZA(II)/Z2)*LAM(II)*X**(ZA(II)/Z2-1 ))
11 CONTINUE

```

```

XOHI = X-SUMFN/SUMFD

```

```

DO WHILE ((ABS(XOHI-X)/XOHI).GT.EPS)

```

```

X = XOHI
SUMFN = 0.0
DO 12 II = 1,NA
SUMFN = SUMFN + (LAM(II)*X**(ZA(II)/Z2))
12 CONTINUE
SUMFN = SUMFN+X-1 0

```

```

SUMFD = 1.0
DO 13 II = 1,NA
SUMFD = SUMFD+((ZA(II)/Z2)*LAM(II)*X**(ZA(II)/Z2-1.))
13 CONTINUE

```

```

XOHI = X-SUMFN/SUMFD

```

```

END DO

```

```

DO 14 II = 1,NA
XXI(II) = LAM(II)*(XOHI**(ZA(II)/Z2))
14 CONTINUE

```

C CALCULATION OF TOTAL INTERFACIAL CONCENTRATION CTI

```

SUMPN = 0.0
DO 15 II = 1,NA
SUMPN = SUMPN+ABS(N(II)*DA(II)*(XXI(II)-XXN(II)))
15 CONTINUE
SUMPN = SUMPN + ABS(NOH*DOH*(XOHI-XBOH))

```

```

SUMPD = 0.0
DO 16 II = 1,NA
SUMPD = SUMPD+ABS(DA(II)*(XXI(II)-XXN(II)))
16 CONTINUE
SUMPD = SUMPD + ABS(DOH*(XOHI-XBOH))

```

P = SUMPN/SUMPD

```
SUMTN = 0.0
DO 17 II = 1,NA
SUMTN = SUMTN + (1.+N(II))*DA(II)*XXN(II)
17 CONTINUE
SUMTN = SUMTN+(1.+NOH)*DOH*XBOH
```

```
SUMTD = 0.0
DO 18 II = 1,NA
SUMTD = SUMTD + (1.+N(II))*DA(II)*XXI(II)
18 CONTINUE
SUMTD = SUMTD+(1 +NOH)*DOH*XOHI
```

```
CTIN = (SUMTN/SUMTD)**(1./(P+1.))*CTO
IF((ABS(CTIN-CTI)/CTIN).GT.EPS)THEN
CTI=CTIN
GO TO 8
```

```
ELSE
CTI = CTIN
ENDIF
```

C CALCULATION OF R_i's OF THE IONS B, C, D, E.

```
DO 19 II = 1,NA
BB(II) = W*(XXI(II)-XXN(II))/(CTI**(-P-1.)-CTO**(-P-1.))
19 CONTINUE
BOH = W*(XOHI-XBOH)/(CTI**(-P-1.)-CTO**(-P-1.))
```

```
DO 20 II = 1,NA
CBN(II) = W*CBA(II)/ZA(II)
20 CONTINUE
```

```
DO 21 II = 1,NA
AA(II) = (ZA(II)*CBN(II)-BB(II)*CTO**(-P))/CTO
21 CONTINUE
AOH = (Z2*CBOH-BOH*CTO**(-P))/CTO
```

```
DO 22 II = 1,NA
CI(II) = W*XXI(II)*CTI/ZA(II)
22 CONTINUE
```

COHI = W*XOHI*CTI/Z2

DO 23 II = 1,NA

R1(II) = DA(II)*((1.-N(II)/P)*(CI(II)-CBN(II))

1 +N(II)*(AA(II)/ZA(II))*(1.+1./P)*(CTI-CTO))

23 CONTINUE

ROH1 = DOH*((1.-NOH/P)*(COHI-CBOH)+NOH*(AOH/Z2)*

1 (1.+1./P)*(CTI-CTO))

SIGR = 0.0

DO 24 II = 1,NA

SIGR = SIGR + ABS(R1(II))

24 CONTINUE

SIGR = SIGR + ABS(ROH1)

SIGD = 0.0

DO 25 II = 1,NA

SIGD = SIGD + ABS(CI(II)-CBN(II))

25 CONTINUE

SIGD = SIGD + ABS(COHI-CBOH)

DRA = SIGR/SIGD

DO 26 II = 1,NA

RA(II) = W*ZA(II)*R1(II)/DRA

26 CONTINUE

RETURN

END

2

VITA

Ashwin P Gramopadhye

Candidate for the Degree of

Master of Science

Thesis: HOMOGENEOUS BED ION EXCHANGE COLUMN MODELS FOR
ULTRAPURE WATER APPLICATIONS AND SIMULATION OF ION
EXCHANGE BEDS IN SERIES

Major Field: Chemical Engineering

Biographical:

Education: Graduated from S.I.E.S. College of Arts and Science, Bombay, India in March 1989; received Bachelor of Engineering degree in Petroleum and Petrochemical Engineering from University of Pune, India in May 1993. Completed requirements for Master of Science degree in Chemical Engineering at Oklahoma State University in December 1996.

Experience: Employed by I.I.T. (Powai), Bombay, India as Research Associate; Oklahoma State University, School of Chemical Engineering as Graduate Teaching Assistant and Graduate Research Assistant; Oklahoma State University, Department of Biosystems and Agricultural Engineering as Graduate Research Assistant and Computer Programmer.